



저작자표시-비영리-변경금지 2.0 대한민국

이용자는 아래의 조건을 따르는 경우에 한하여 자유롭게

- 이 저작물을 복제, 배포, 전송, 전시, 공연 및 방송할 수 있습니다.

다음과 같은 조건을 따라야 합니다:



저작자표시. 귀하는 원저작자를 표시하여야 합니다.



비영리. 귀하는 이 저작물을 영리 목적으로 이용할 수 없습니다.



변경금지. 귀하는 이 저작물을 개작, 변형 또는 가공할 수 없습니다.

- 귀하는, 이 저작물의 재이용이나 배포의 경우, 이 저작물에 적용된 이용허락조건을 명확하게 나타내어야 합니다.
- 저작권자로부터 별도의 허가를 받으면 이러한 조건들은 적용되지 않습니다.

저작권법에 따른 이용자의 권리는 위의 내용에 의하여 영향을 받지 않습니다.

이것은 [이용허락규약\(Legal Code\)](#)을 이해하기 쉽게 요약한 것입니다.

[Disclaimer](#)

Thesis for the Degree of Master of Technology

**Synthesis and optical properties of
two-dimensional lead halide
perovskite $(\text{C}_6\text{H}_5\text{CH}_2\text{NH}_3)_2\text{PbBr}_4$**

by

Fanfan Zhu

Interdisciplinary Program of Biomedical, Mechanical &
Electrical Engineering
The Graduate School

Pukyong National University

February 2019

**Synthesis and optical properties of
two-dimensional lead halide
perovskite $(\text{C}_6\text{H}_5\text{CH}_2\text{NH}_3)_2\text{PbBr}_4$**

이차원 페로브스카이트 $(\text{C}_6\text{H}_5\text{CH}_2\text{NH}_3)_2\text{PbBr}_4$ 의

합성과 광학적 특성

Advisor: Prof. Hyo Jin Seo

By

Fanfan Zhu

A thesis submitted in partial fulfillment of the requirements
for the degree of

Master of Engineering

in Interdisciplinary Program of Biomedical, Mechanical &
Electrical Engineering, The Graduate School,

Pukyong National University

February 2019

**Synthesis and optical properties of
two-dimensional lead halide perovskite**



A dissertation

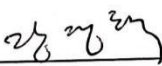
by

Fanfan Zhu

Approved by:



(Chairman) Professor Cheol Woo Park



(Member) Ph.D. Kyoung Hyuk Jang



(Member) Professor Hyo Jin Seo

February 2019

Contents

| | |
|--|----|
| 1.Introduction..... | 1 |
| 1.1.Crystal Structure and Quantum Trap of Organic/Inorganic Hybrid Perovskites..... | 4 |
| 1.1.1.Crystal structure | 4 |
| 1.1.2.Quantum well structure..... | 8 |
| 1.2.Preparation of organic/inorganic hybrid perovskite materials | 14 |
| 1.2.1.Single crystal preparation | 14 |
| 1.2.2.Film preparation technology | 17 |
| 1.3.Application of organic/inorganic hybrid perovskite materials | 22 |
| 1.3.1.Application on light emitting diodes (LEDs)..... | 22 |
| 1.3.2.Applications on field effect transistors (FETs) | 26 |
| 1.3.3.Applications on photovoltaic devices | 28 |
| 1.3.4.Other applications | 30 |
| 1.4.The purpose and significance of the research | 31 |
| 2.Background: Synthesis and Characterization of Organic/Inorganic Hybrid Perovskite Materials Based on Lead Iodide | 34 |
| 2.1.Introduction | 34 |
| 2.2.Experimental part | 36 |
| 2.2.1.Chemical reagents..... | 36 |
| 2.2.2.Preparation of organic amine salts | 36 |
| 2.2.3.Preparation of organic/inorganic hybrid calcium ore materials | 37 |
| 2.2.4.Characterization means | 39 |
| 2.3.Spectroscopic measurement..... | 40 |
| 2.3.1.Analysis of the structure of hybrid perovskite materials | 40 |
| 2.3.2.UV-Vis absorption spectroscopy analysis of hybrid perovskite films | 44 |
| 2.3.3.Fluorescence (PL) spectral analysis of hybrid perovskite films | 46 |
| 3.Sample preparation and Discussions | 50 |
| 3.1. Sample preparation | 50 |
| 3.2. Results and discussions..... | 51 |
| 4.Conclusions..... | 62 |

Acknowledgements.....63
References.....64



Synthesis and optical properties of two-dimensional lead halide perovskite



Fanfan Zhu

Interdisciplinary Program of Biomedical, Mechanical & Electrical Engineering

Pukyong National University

Abstract

In this work, $(\text{C}_6\text{H}_5\text{CH}_2\text{NH}_3)_2\text{PbBr}_4$ were prepared by chemical method. The crystalline phase was confirmed by X-ray powder diffraction analysis. The morphology of the materials was analyzed by scanning electron microscopy (SEM), indicating a good crystallization. The luminescence properties such as photoluminescence spectra and decay curves were investigated. Low and high temperature photoluminescence spectra show the coexistence of free exciton and self-trapped exciton luminescence in a deformable lattice. The thermal stabilities were investigated from the temperature dependent luminescence decay curves (lifetimes) and spectra intensities. The obtained $(\text{C}_6\text{H}_5\text{CH}_2\text{NH}_3)_2\text{PbBr}_4$ perovskite reported here can be applied to other two-dimensional

perovskites to increase the optoelectronic efficiency of the device in the future.



1. Introduction

In recent years, organic/inorganic hybrid chemicals have made great progress in the neighborhood of optoelectronic functional materials due to their unique structure, and have a very broad application prospect. ^[1-10]

The innovation of advanced technology and the requirement of electronic market are always focusing on low cost electronics, easy processing, having enhanced performance. Take as an example the improvement of flat panel display. It has experienced three periods: CRT (Cathode Ray Tube), LCD (Liquid Crystal Display) and OLED (Organic Electronic-luminescence Display). CRT has been replaced by LCD and OLED because the depth and weight of CRTs are not appropriate for portable applications. ^[11-16] The organic materials are more and more widely used due to their various advantages: low temperature processing, flexibility of organic chemistry to form molecules, good luminescent properties. However, organic compounds generally have a number of disadvantages, including poor thermal stability, as well as a limited mobility at room temperature. ^[17-20]

Besides the inorganic semiconductors and the organic materials, an

interesting class of materials is intensively studied: the hybrid materials, which are expected to combine the attractive features of organic materials and inorganic materials within a single molecular-scale composite, and can be synergistically exploited to overcome the limitations when the two kinds of materials are used separately. In the past two decades, the organic-inorganic hybrid perovskites have arisen as a new functional material and have drawn great attention and research effort^[21-25]. When deposited by spin-coating, these compounds are self-assembled systems. They form a multi-quantum well structure spontaneously and exhibit excellent optical and electronic properties at room temperature. Their optical properties can be finely tuned thanks to molecular engineering on the organic part or on the inorganic part. Furthermore, spin-coating is a very simple method, compared to the deposition techniques for inorganic semiconductors, such as MBE (Molecular Beam Epitaxy), MOCVD (Metalorganic Chemical Vapor Deposition) and PECVD (Plasma Enhanced Chemical Vapor Deposition).

Recently, organic-inorganic hybrid perovskites have used in many research and practical fields such as surface plasmons, Symonds et al. (2007,2008) LEDs, Era et al. (1994) solar cells Kojima et al. (2009); Li et al. (2010) ;

Koutsclas et al. (2011) as well as microcavities. Brédier et al. (2006); Lantý et al. (2008b); Wei et al. (2012) Especially the use of this hybrid semiconductor inside microcavities could open the way to realize polariton laser at room temperature. The team “Optical Properties of Hybrid Nanostructures” of LPQM ENS Cachan has successfully realized microcavities containing two dimensional layered organic-inorganic perovskites, working in the strong coupling regime at room temperature, and emitting in the green, blue and near UV range. Additionally, some hybrid vertical microcavities containing a layer of inorganic semiconductors such as GaN or ZnO and a perovskite layer have been performed, and the strong coupling regime between the photon mode and the two excitons has been demonstrated at room temperature. Although perovskites show stronger excitonic properties and brighter luminescence than inorganic semiconductors, and stronger thermal- and photo-stability than most organic Semiconductors, it is still quite urgent to work on optical optimization of perovskite layers, especially the long time photo-stability, in order to support higher requirements of technological and scientific applications. ^[26-28]

These important issues bring about the research subject of this thesis. The objectives are to synthesize, characterize and optimize new functionalized organic-inorganic hybrid perovskites for the application of

microcavities, and further scientific and practical requirements. In this manuscript, we focus our attention on the group of two-dimensional (2D) layered lead halide perovskites and emphatically make research efforts on several aspects: Improvement of optical properties; Study on photostability; and Application of perovskite layers in microcavities.

1.1. Crystal Structure and Quantum Trap of Organic/Inorganic Hybrid Perovskites

1.1.1. Crystal structure

The typical perovskite structure compound of can be expressed as AMX_3 , as shown in Figure 1.1, where M is a metal cation that can coordinate to form an octahedron (can be composed of more than 50 elements such as Ti, Fe, Nb, etc.), X is an anion capable of forming a coordination octahedron with A (may be composed of elements such as Cl, Br, and I), and A is a metal cation which can balance M and anion charge to make the system electrically neutral (acceptable by Ca, Ba, Sr, Pb, K, Se, Y and 20 kinds of elements such as lanthanum metal from La to Lu are formed) ^[29].

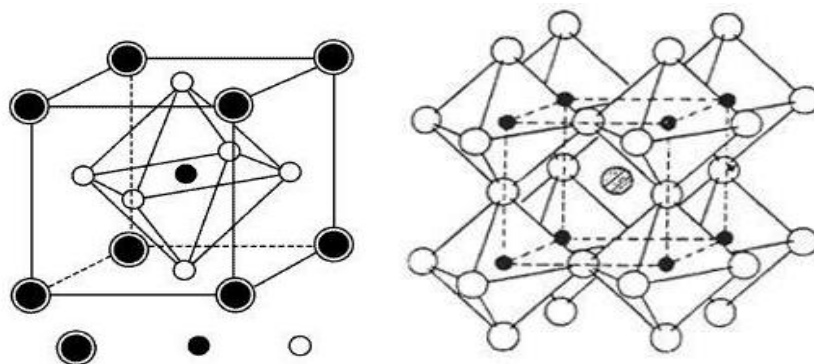


Fig. 1.1 (a) Ball-and-stick model of the basic perovskite structure and (b) their extended network structure connected by the corner-shared octahedra.

The organic/inorganic hybrid perovskite is a derivative of cubic perovskite (AMX_3). At this time, A is an organic ammonium cation, and the metal cation M^{2+} and an anion X^- (usually a halogen) form an inorganic octahedral structure MX_6^{4-} through a strong coordinate bond, M is located in the body of the halogen octahedron, and X is co-topped with the octahedral apex. The mode is connected and extends infinitely in the direction of the three-dimensional space to form a network-like frame structure: the organic ammonium cation A is filled in the void formed by the co-topped octahedron, as shown in Fig. 1.2a. If the three-dimensional (3D) hybrid perovskite structure is cut into a sheet along a certain crystal plane orientation, the sheet structure can be regarded as a two-dimensional

(2D) layered perovskite structure. According to the crystal plane orientation, it can be divided into three types: $\langle 100 \rangle$, $\langle 110 \rangle$ and $\langle 111 \rangle$. The simplest and most common structure is $\langle 100 \rangle$ oriented hybrid perovskite, and its general formula is $(\text{RNH}_3)_2\text{A}_{n-1}\text{X}_{3n+1}$. Here, RNH_3^+ is an aliphatic (linear) or aromatic organic ammonium cation, while A includes monovalent cation (CH_3NH_3^+ , K^+ , Na^+), and M is mainly IVA metal ion (Pb^{2+} , Sn^{2+} , Ge^{2+}) as well as monovalent cation such as Cu^{2+} , Ni^{2+} , Co^{2+} , Fe^{2+} , Mn^{2+} , Pd^{2+} , Cd^{2+} and Eu^{2+} .

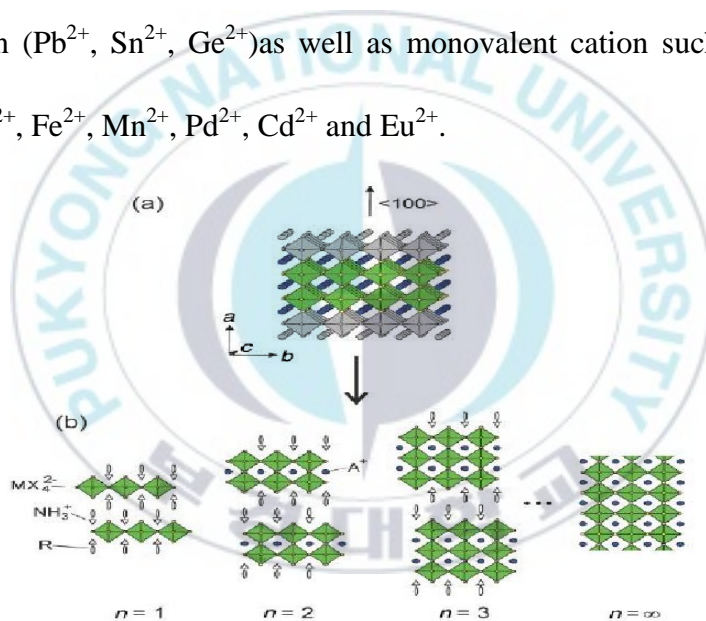


Fig. 1.2 (a) Polyhedral representation of the 3D hybrid perovskite AMX_3 structure along the $\langle 100 \rangle$ direction. (b) The $\langle 100 \rangle$ -oriented hybrid perovskite series by alternating stacking inorganic layers with organic cations with general formula of $(\text{R-NH}_3)_2(\text{CH}_3\text{NH}_3)_{n-1}\text{MnX}_{3n+1}$. The thicknesses of inorganic slabs increase and toward 3D structure with increasing n .

The <100> oriented hybrid perovskite is a multiple quantum structure hydrazine crystal material (hereinafter, hybrid perovskites are specifically referred to as <100> type hybrid perovskites). when $n=1$ hybridization, the perovskite is of the formula $(\text{RNH}_3)_2\text{MX}_4$, where the organ ammonium cation is a monogamic ammonium cation or a bis-organ ammonium cation ($\text{NH}_3^+-\text{R}-\text{NH}_3^+$), and the halide ion of the inorganic sheet layer is formed, and the ammonium end of the organic chain is connected to the inorganic octahedron by strong hydrogen bonding (**Fig. 1.2b**). The bilayer structure of the monoammonium cation is connected by Van der Waals force, and the tail end extends to the adjacent. In the void of the inorganic layer, an organic layer is formed: the two NH_3 groups of the head and the tail of the bis-organic amine are bonded to the halogen of the adjacent inorganic layer, so that the organic layer is a monomolecular layer, and the organic layer and the inorganic layer alternate with each other to form a stable single layered inorganic sheet layer of hybrid perovskite structure.^[30]

When $n \geq 2$, the short-chain A organic cation (usually CH_3NH_3^+) is filled in the void of the inorganic layer of the inorganic metal halogen octahedral structure, and is bonded to the inorganic layer by hydrogen

bonding to function like a glue. The inorganic octahedral layer structure is tightly bonded together to form a structure of a multi-inorganic sheet layer, and the relative number of methylamine can adjust the number n of the inorganic sheet layer, that is, the thickness of the inorganic layer can pass through the amount of methylamine^{31,32}. In the hybrid calcium ore of the multi-layer inorganic layer, the long-chain organic ammonium cation forms an organic layer through hydrogen bonding and van der Waals force (the combination is similar to the case of $n=1$), and finally, more product of alternating layers of calcium minerals and organic components (**Fig. 1.2b**).

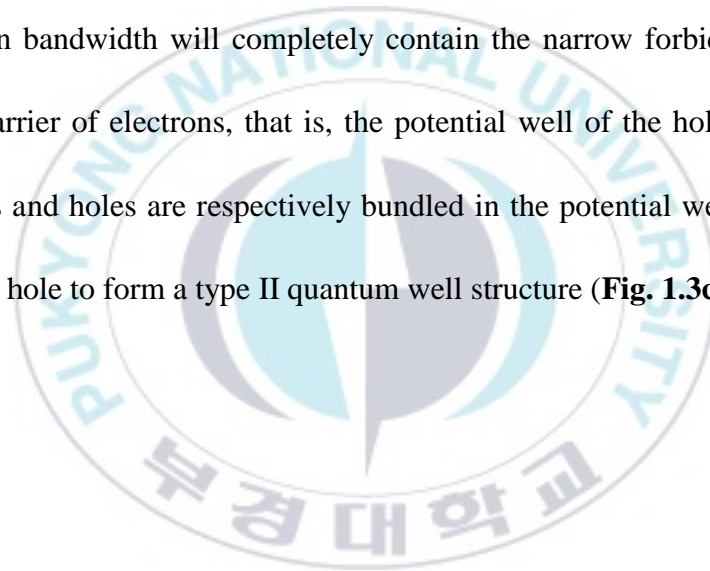
When $n=\infty$, the content of the organic cation of the short chain is much larger than that of the long chain organic cation, and therefore, it is substantially filled with the short organic ammonium chain by hydrogen bonding, and is filled in the void of the inorganic metal halide octahedral structure to form an extension in each orientation.

1.1.2. Quantum well structure

Since the organic component and the inorganic component are alternately stacked, a layered organic/inorganic hybrid perovskite is

formed, so that such a structure has the characteristics of a quantum structure, as shown in **Fig. 1.3**. Usually there are three kinds of multi-quantum negative structures. Due to the difference in the bands of the organic matter and the inorganic matter (the position of the energy level), the conduction band of the inorganic layer is lower than the conduction band of the organic layer (the lowest empty orbit LUMO), and the valence band of the inorganic layer is higher than the valence band of the organic layer (The highest occupied orbit HOMO), so that the forbidden band of the organic layer (HOMO-LUMO energy gap) is larger than the inorganic layer (**Fig. 1.3a**). The inorganic layers are potential wells, and the organic layer acts as a barrier; on the contrary, if the forbidden band width of the inorganic layer is larger than the forbidden band width of the organic layer, then the forbidden band of the organic layer will be affected by the inorganic layer. The forbidden band is completely inclusive, for that the inorganic layer is a potential barrier, and the organic layer is a potential well (**Fig. 1.3b**). In these two forms, the forbidden band of one layer completely falls into the forbidden band of another layer, and electrons and holes are bundled. In the same layer (organic or inorganic layer), therefore, the two structural portions are

called I-type quantum structures, and when the inorganic layer and the organic layer have a forbidden band width not large, the forbidden band of the inorganic layer and the organic layer are not aligned, and the HOMO and LUMO bands of the organic layer are higher (or lower) than the valence and conduction band of the inorganic layer, and the layer with a small forbidden band will serve as an electron potential well. The layer of forbidden bandwidth will completely contain the narrow forbidden band as the barrier of electrons, that is, the potential well of the hole, and the electrons and holes are respectively bundled in the potential well and the potential hole to form a type II quantum well structure (**Fig. 1.3c**).



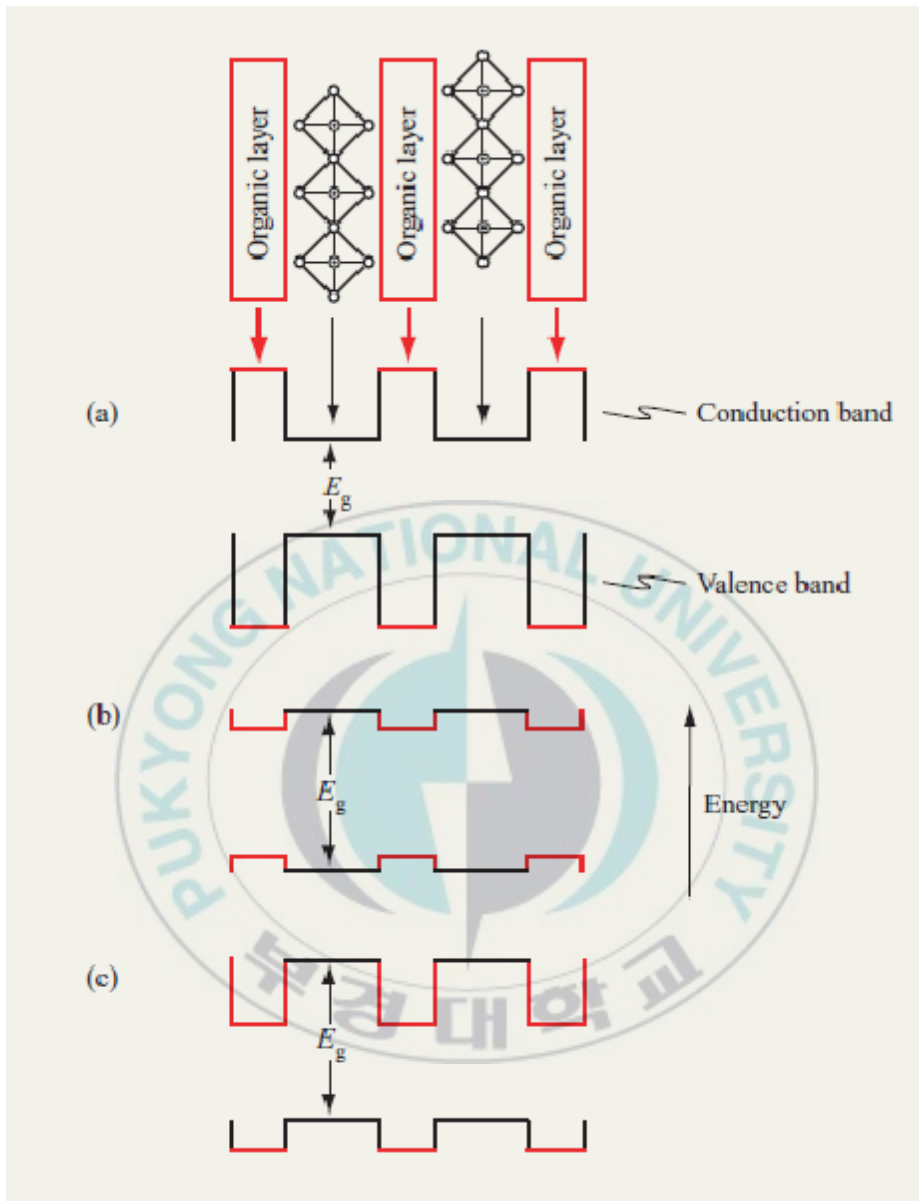


Fig. 1.3 Schematic organic or inorganic perovskite structure and possible energy-level schemes. The most common arrangement is shown in (a), semiconducting inorganic sheets alternate with organic layers having much wider bandgaps, resulting in a type I quantum well structure. In (b), wider bandgap inorganic layers and organic cations with a smaller

HOMO-LUMO gap results in another type I quantum well structure. In (c), by shifting the electron affinity of the organic layers relative to the inorganic layers, a staggering of energy levels results in a type II quantum well structure.

The organic element machine has a strong optical absorption under the chamber, which is closely related to the exciton (excited electron-hole pair) energy state of the semiconductor inorganic layer. In general inorganic semiconductor materials, the exciton binding energy is very high. Usually, only at very low temperatures, photoluminescence can be observed in high-purity crystals^[33]. And in quantum materials, especially in the structure of I-type quantum wells, excited electrons and holes are bound. In the inorganic layer (potential well), the diffusion of excitons will be limited by the organic barrier layer, and the excitons are bound in a very narrow well layer, making the combination of electrons and holes easier. Therefore, the material has a large exciton binding energy. According to the classical quantum confinement effect theory, in the two-dimensional quantum well structure, the exciton binding energy is generally four times that of the bulk material. The titanium ore multi-quantum well crystal has a very high exciton binding energy, which is much higher than four times

the exciton binding energy of the bulk material.^[34]

Through theoretical calculations and experiments, it has been found that the difference in dielectric between the organic layer (barrier layer) and the inorganic layer (potential layer) has a large influence on the exciton binding energy. In the hybrid perovskite structure, the dielectric constant of the inorganic substance is larger, and the dielectric constant of the organic substance is lower. The organic layer having a smaller dielectric constant is added to the inorganic layer having a larger dielectric constant, and the organic layer is reduced. The shielding effect of electrons and holes in the inorganic well layer increases the coulomb interaction of electron-hole bonding, thus making the hybrid perovskite have greater exciton binding energy. This phenomenon is called dielectric confinement. The effect is that as the ratio of the dielectric constant of the inorganic component to the organic component increases, the exciton binding energy increases.

The dual role of the dielectric confinement effect and the two-dimensional quantum well confinement effect makes the inorganic hybrid perovskite materials having very prominent optoelectronic properties, such as higher exciton binding energy, and large vibrator

strength, strong room temperature photoluminescence, nonlinear optical properties, strong exciton-photon coupling phenomena, etc.

1.2. Preparation of organic/inorganic hybrid perovskite materials

The driving forces for self-assembly in the formation of organic/inorganic hybrid perovskite materials are coordination bonds (formation of MX_6^{4+} metal halide octahedron), hydrogen bonding (interaction of halides in organic cations and inorganic layers), van der Waals forces or ruthenium stacking (weak interaction between organic cationic groups) and the like.

1.2.1. Single crystal preparation

The analysis and testing of single crystals is the most direct and most detached means of studying the crystal structure of materials and the physical energy of materials. Therefore, the preparation of a single crystal having a regular shape has a non-essential significance, and typical methods include a solution cooling method, an evaporation solvent method, a gel method, and a layered solution method.

1.2.1.1. Solution cooling method

The growth of single crystals (polycrystals) by solution method is currently the most common method for preparing organic/inorganic hybrid perovskite crystals. For a single layer of inorganic sheet of hybrid perovskite crystals, a certain stoichiometric ratio of metal halides and organic amines can be dissolved in a solvent, and the two solvents are mixed at a higher temperature to completely dissolve them. By controlling the cooling rate and slowly cooling to room temperature (or below), the hybrid perovskite crystals can be precipitated. By changing the stoichiometric ratio of the metal halide and the organic amine, the number of the perovskite inorganic layer can be controlled, resulting a hybrid perovskite crystal of a multilayer inorganic sheet. The limitation of this method is that it is necessary to find a co-solvent capable of simultaneously dissolving metal halides and organic amine salts, and the divalent cation of a rare earth metal is very compatible with the solvent, such as Eu^{2+} , thus, it avoids generating impurities. ^[35, 36]

1.2.1.2. Evaporation solvent method

The evaporative solvent method is similar to the solution method except that the evaporative solvent method is a process of driving

crystallization by evaporating the solvent at a slow rate, instead of using a step temperature to cool down. The crystal quality obtained by this method is lower than that of the solution method, and the solvent is evaporated for a long time (usually several weeks or more). However, the time for culturing a single crystal can be shortened by using a mixed solvent. For example, Hattori T. uses a mixed solvent of acetone and nitromethane in a volume ratio of 1:2 to grow a crystal of $(\text{C}_6\text{H}_5\text{C}_2\text{H}_4\text{NH}_3)_2\text{PbCl}_4$.

1.2.1.3. Gel method

When the organic component and the inorganic component are not dissolved in a solvent, we can dissolve the two components in different solvents separately, and use the gel method to slowly expand the two solutions to obtain a single crystal. Guan J. and Suib S.L. et al. have reported that a larger single crystal has been obtained by a gel method.

The single crystal obtained by this method has a high optical quality and a large size, but has a long slicing cycle. And the biggest disadvantage is that the composition of the gel usually contaminates the single crystal product.

1.2.1.4. Layered solution method

The layered solution method is also a very good method when the cosolvents of the organic and inorganic components are not well found, and the organic and inorganic components are separately dissolved in two solvents (the two solvents have a certain mutual solubility). If density difference is more obvious, the less dense solution is carefully and slowly added to the liquid layer of the denser solution. Because of the density difference between the two solutions, the stratification phenomenon is obvious, and between the two solutions a clear interface occurs, and the inorganic and organic components diffuse very slowly. After a long period of time, crystals of larger size can be grown at the interface. D. B. Mitzi et al. prepared a $(\text{C}_6\text{H}_5\text{C}_2\text{H}_4\text{NH}_3)\text{PbCl}_4$ crystal using a layered solution.

1.2.2. Film preparation technology

Many electronic and optical devices are fabricated and assembled using thin films, so suitable thin film preparation techniques are important for obtaining high quality optoelectronic functional devices. There are many film preparation techniques for hybrid materials, such as spin coating, vacuum heat source deposition, multilayer film technology, and

patterned thin film technology.

1.2.2.1. Spin coating method

Spin coating technology is widely used in the optoelectronic industry. The thin film device is prepared by this method, and the cost is low, simple and convenient. The sol (solution) is dropped on the substrate, and the disk is rotated to cause most of the colloid (solution) to be pulled out by centrifugal force. And a small amount of the colloid (solution) remaining on the substrate is under the action of surface tension and centrifugal force. Gradually develop to form a uniform film. Due to the dissolution or dispersion of the material into a sol, the choice of solvent is difficult, which limits the application range of spin coating to some extent.

Due to its excellent film-forming properties, hybrid perovskites can be spin-coated on different substrates, such as glass, quartz, silicon wafers and plastics. Generally, it is easy to find a suitable solvent, so spin coating method is the most common method of hybridizing perovskites.

1.2.2.2. Vacuum heat source deposition

The layered hybrid perovskite can be obtained by vacuum deposition of a dual heat source, such as first depositing a metal halide on a substrate

by vacuum deposition or spin coating, and then placing the substrate in an organic ammonium salt. In the solution, the evaporation rate and the pressure ratio are controlled, and the organic-inorganic composite can be simultaneously deposited on the quartz substrate to obtain a crystallized perovskite film. This technique is especially suitable for situations where the organic and inorganic components lack a common solvent. Different materials have different evaporation rates, and the heating parameters can be adjusted to obtain different organic-inorganic hybrid systems. Single heat source ablation (SSTA) technology is a good alternative for dual heat source deposition. Both the organic and inorganic components are placed in the same enamel heater in the vacuum chamber. When a large current is passed through the heater, the organic and inorganic materials are evaporated and deposited into the lining in a very short time (<1 s) on the bottom. The perovskite film obtained by this method has high quality and provides a good process and technical guarantee for preparing high-performance optoelectronic devices such as field effect transistors and light-emitting diodes. The shortcoming is that this method has higher requirements for the vacuum environment.

1.2.2.3. Multilayer film technology

Mitzi et al. invented the insertion method (two-step impregnation method), and the metal halide MI₂ was first deposited on the substrate by vacuum deposition, immersed in the organic ammonium salt solution at room temperature for a short period of time (1-5 min), and the organic molecule was inserted. In the inorganic framework, a new single-phase hybrid perovskite film is formed. Conversely, the organic ammonium salt is immersed in the metal halide solution, and a layered hybrid perovskite can also be formed. For example, by inserting an inorganic salt into a solution of a long-chain alkyl ammonium salt, a double-structured hybrid perovskite can be formed on the substrate.

Multilayer film self-assembly (LBL) that is, alternately using the insertion method, the hybrid perovskite is immersed in an organic solution or a metal halide solution, which can be used for preparing a multi-layered hybrid perovskite film, and more The method controls the film thickness. Multi-layer membrane technology is simple and quick, easy to find a suitable solvent, and can easily control the thickness of the film, but it is difficult to find a good solvent for organic matter but poorly soluble for inorganic substances (or easy to dissolve for inorganic substances).

1.2.2.4. Patterned film technology

Large-area patterning of organic functional materials is a very important step in integrated organic optoelectronic devices. In recent years, etching organic semiconductor materials by photolithography to obtain micron or submicron size pattern structures has attracted widespread attention. When organic/inorganic hybrid perovskites are used as channel layers for field effect transistors (FFTs), luminescent layers for LED devices, or photovoltaic materials, they require patterning, which is compatible with solution-based production processes.

The insulating strip pattern of the hybrid perovskite material $(\text{CH}_3\text{C}_2\text{H}_4\text{NH}_3)_2\text{PbI}_4$ can be prepared by capillary micro molding (MIMIC) method. The grooved polydimethylsiloxane (PDMS) mold is placed on the Si substrate. The channel and the substrate of the mold form capillary microtubes. Under the driving of capillary force, the precursor solution is introduced into the channel: the solvent is evaporated, the mold is removed, and the pattern of $(\text{CH}_3\text{C}_2\text{H}_4\text{NH}_3)_2\text{PbI}_4$ remains on the substrate. A striped green fluorescent pattern of perovskite can be observed under the microscope (**Fig. 1.4a**). The anti-wetting technique and polymer bonding technology can be combined to successfully prepare the

insulating tetragonal $(\text{CH}_3\text{C}_2\text{H}_4\text{NH}_3)_2\text{PbI}_4$. The microstructure was successfully transferred to a glass substrate. Fluorescence at room temperature is shown in **Fig. 1.4b**.

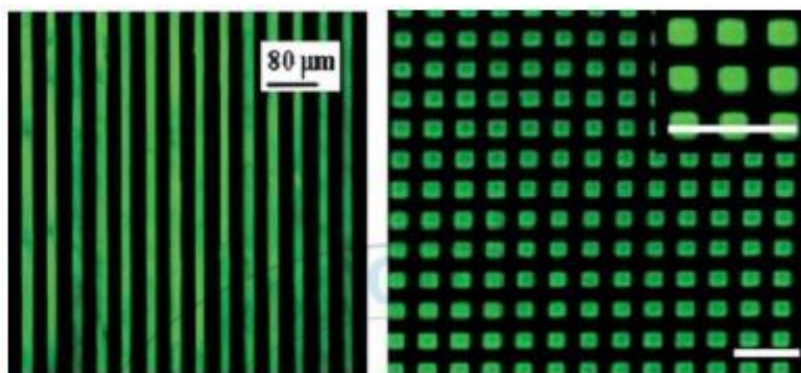


Fig. 1.4(a) Fluorescent optical micrograph of the patterned $(\text{CH}_3\text{C}_2\text{H}_4\text{NH}_3)_2\text{PbI}_4$ film on Si substrate. The green stripes correspond to the luminescence of $(\text{CH}_3\text{C}_2\text{H}_4\text{NH}_3)_2\text{PbI}_4$ excited by Hg lamp and the black stripes are the bare substrate, **(b)** The isolated pattern of luminescence $(\text{CH}_3\text{C}_2\text{H}_4\text{NH}_3)_2\text{PbI}_4$ under fluorescent microscope prepared by solvent-assisted de-wetting and polymer-bonding lithography.

1.3. Application of organic/inorganic hybrid perovskite materials

1.3.1. Application on light emitting diodes (LEDs)

The unique multi-quantum well structure of the hybrid perovskite

material provides outstanding photoelectric properties with good stability and photoluminescence at room temperature. Hybrid perovskite materials can be used as luminescent materials in the LED field. For example, PbBr_2 and $\text{C}_6\text{H}_3\text{C}_2\text{H}_4\text{NH}_2$ can be used to prepare blue $(\text{C}_6\text{H}_5\text{C}_2\text{H}_4\text{NH}_2)\text{PbI}_4$; PbI_2 and $\text{C}_6\text{H}_3\text{C}_2\text{H}_4\text{NH}_2$ can be used to prepare green $(\text{C}_6\text{H}_5\text{C}_2\text{H}_4\text{NH}_2)\text{PbBr}_4$; and $\text{C}_n\text{H}_{2n+1}\text{NH}_2$ and MnCl_2 Preparation of red light $(\text{C}_n\text{H}_{2n+1}\text{NH}_3)_2\text{MnCl}_4$ ($n=1-3$)^[37-40].

The IVA group metal halide hybrid material is used in thin film heterojunction devices due to high carrier mobility, strong photoluminescence and excellent processing properties, and may have electroluminescence properties.

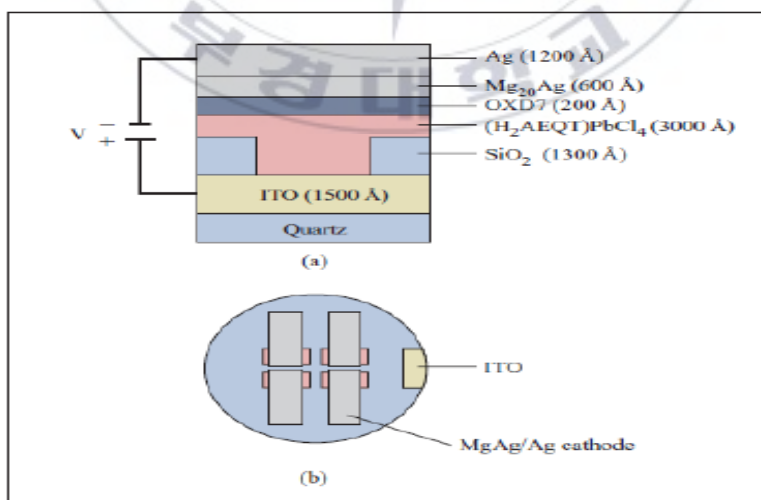


Fig.1.5 The cross section of OILED device structure

Era et al. prepared high-efficiency organic-inorganic light-emitting diodes (OLEDs). They prepared $(C_6H_5C_2H_4NH_2)PbI_4$ thin film materials by simple spin coating method and used them as light-emitting layers. Oxadiazole was an electron transport layer, ITO and Mg. -Ag alloy is a positive and negative electrode, the diode emits green light with a wavelength of 520 nm, the driving voltage is 24 V, and the illuminance reaches 10000 cd m^{-2} at a current density of 2 A cm^{-2} and liquid nitrogen temperature. When it is raised to room temperature, its luminescence intensity drops rapidly to 1/10 of the liquid chlorine temperature due to thermal quenching of excitons, etc. Therefore, in order to prevent excitons from being quenched by heat, the excitons in the compound are stabilized. To increase the intensity of room temperature electroluminescence, it is necessary to use an optically active chromophore group with a relatively complex structure instead of an optically inert alkyl group or a simple aromatic moiety.^[41, 42]

In order to prepare a more stable hybrid perovskite material with normal temperature excitons, Mitzi et al. synthesized a novel thiophene oligomer-containing AEQT molecule and deposited it on ITO-coated quartz substrate by single source thermal etching (H_2AEQT) $PbCl_4$ film,

they use (H₂AEQT)PbCL₄ film as the light-emitting layer, oxadiazole is the electron transfer layer, ITO and Mg-Ag alloy are the positive and negative electrodes, and the organic/inorganic light-emitting diode (OILER) with better performance is prepared. (Fig. 1.5), yellow-green light with a wavelength of 530nm can be emitted at room temperature, the large luminous efficiency is 0.1lm/w, the power conversion efficiency is 0.11% and (AEQT)_n(AETH)1 is selected. -nPbBr₄ is used as an active layer, wherein n is the molar concentration of AEQT in the organic mixture component, AETH is an optically inert dye; the smaller the optically active dye concentration n, the higher the fluorescence quantum efficiency, and the highest fluorescence when n=2% The quantum efficiency is 9%.

The organic/inorganic hybrid perovskite material can adjust the energy band structure of the material through different inorganic components or organic components to achieve various color-developing electroluminescent devices. The excellent film-forming properties of hybrid perovskite materials have great development prospects in achieving full-color display and white LED.

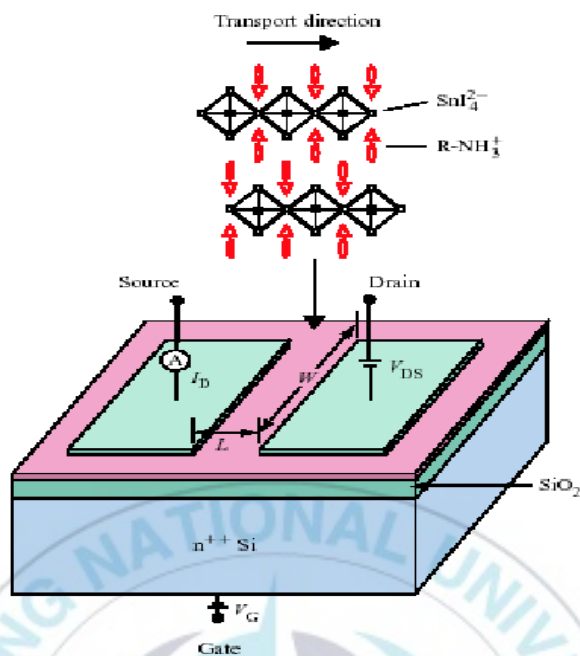


Fig. 1.6 The structure diagram of the FETs by organic/inorganic hybrid perovskite materials as channel layer

1.3.2. Applications on field effect transistors (FETs)

Since the organic/inorganic hybrid perovskite material has high carrier mobility, and the carrier transport performance and energy band structure are adjustable, the film deposition is simple and low-cost, so the application on the field effect transistor is particularly cited. People pay attention.^[43]

Mitzi et al. prepared a field effect transistor (FET) of the first

organic/inorganic hybrid perovskite structure, as shown in **Fig. 1.6**. The $(\text{C}_6\text{H}_5\text{C}_2\text{H}_4\text{NH}_3)_2\text{SnI}_4$ film obtained by spin coating was used as a transmission layer of a field effect transistor, n-type Si was used as a gate material, SiO_2 was used as a gate insulating layer, and Pt (Au) was used as a source and drain metal material. The field-effect mobility of this transistor reaches $0.61 \text{ cm}^2 \cdot \text{V}^{-1} \cdot \text{s}^{-1}$ and the switching ratio reaches 10^6 . Its performance is good, comparable to amorphous silicon or the best organic semiconductor fabricated FETs.

However, Sn^{2+} is easily hydrolyzed and oxidized. The hybrid perovskite material $(\text{C}_6\text{H}_5\text{C}_2\text{H}_4\text{NH}_3)_2\text{SnI}_4$ is very unstable in air and completely degraded in a few hours. The film changes from red to colorless, from material synthesis to device processing and assembly, operating in an inert atmosphere. Therefore, in order to overcome the instability of the Sn-like hybrid perovskite material in the air, and improve stability, Mitzi et al. further improved the $(\text{C}_6\text{H}_5\text{C}_2\text{H}_4\text{NH}_3)_2\text{SnI}_4$ film by low-temperature melting method, and The mixture of SiO_2 and polyimide is used as the gate insulating layer material, and the film material obtained by this method has better performance. The stability of the hybrid material and the mobility of the device are improved, and the polyimide film is

improved. To a certain extent, it has played a role in packaging. The film can be stabilized in air for more than 72 h, and the mobility reaches $1.7\text{cm}^2 \text{V}^{-1} \text{s}^{-1}$, and the switching ratio is 10^6 .

In addition, in the layered framework composed of the metal halide of the hybrid perovskite, an aromatic organic amine having a conjugated structure is introduced, and the π - π conjugation effect enables the organic layer to have overlapping electron channels. Participate in electron transport to improve the electrical properties of materials and improve carrier mobility.

1.3.3. Applications on photovoltaic devices

Organic/inorganic hybrid perovskite materials are useful as sensitizing materials for photovoltaic devices. $\text{CH}_3\text{NH}_3\text{PbBr}_3$ and $\text{CH}_3\text{NH}_3\text{PbI}_3$ are used as photo sensitizers, and TiO_2 (n-type semiconductor) constitutes a co-excited heterojunction system. First, a dense TiO_2 is grown on the FTO conductive glass as a hole blocking layer. A mesoporous TiO_2 film was prepared as an electron acceptor and electron transport layer, and then the p-type hybrid perovskite material was self-assembled onto the mesoporous TiO_2 film by spin coating to form an electron donor and a

photosensitizing material. The anode of the battery is finally assembled into a complete photoelectrochemical cell using a cathode of PTO-coated FTO glass in an I/I-ethylene solution. The electrodes are separated by a 50 μm thick separator. The prepared battery is ideal. The effect, as shown in Table 1.1, the photoelectric conversion rate of $\text{CH}_3\text{NH}_3\text{PbBr}_3$ sensitized photocell reached 3.8%.

Table 1.1 The solar cells parameters of organic/inorganic hybrid perovskite

| Perovskite sensitizer on TiO_2 | J_{sc} (mA/cm^2) | V_{oc} (V) | FF | η (%) |
|---|---|---------------------|------|------------|
| $\text{CH}_3\text{NH}_3\text{PbBr}_3$ | 5.57 | 0.96 | 0.59 | 3.13 |
| $\text{CH}_3\text{NH}_3\text{PbI}_3$ | 11.0 | 0.61 | 0.57 | 3.81 |

The band structure, absorption spectrum range and exciton binding energy of organic/inorganic hybrid perovskite materials are designed and artificially adjustable, which provides a new idea for the application of hybrid perovskite materials. It can be expected that such materials have great application prospects in photovoltaic solar energy.

1.3.4. Other applications

Organic/inorganic hybrid perovskite materials such as $(\text{C}_6\text{H}_5\text{C}_2\text{H}_4\text{NH}_3)_2\text{PbBr}_4$ and $(\text{C}_3\text{H}_7\text{NH}_3)_2\text{PbBr}_4$ can be used as scintillators for X-ray synchrotron radiation, nuclear resonance scattering, etc., and experimental studies have shown that they are in the fields of industry, medical treatment, etc. There is a wide range of applications. Scintillators are used to detect ion (proton) radiation, an optical material that converts radiant energy into visible light. The ideal scintillation material should have high light conversion efficiency, fast response speed and good radiation damage resistance. The usual organic scintillation has a fast response speed, but the quantum conversion efficiency is low, resulting in a weak fluorescent signal, which reduces the detection test. Accuracy, while inorganic scintillators have large quantum conversion efficiencies, their decay times are typically in the microsecond range, much higher than organic scintillators, thus limiting the use of inorganic scintillators. ^[44, 45]

Shibuya K. et al. proposed that the organic/inorganic hybrid perovskite $(\text{C}_6\text{H}_{13}\text{NH}_3)_2\text{PbI}_4$ has high exciton radiation efficiency and fast response time (in the order of picoseconds), and has good resistance to radiation damage, which will be a very A good scintillating material that meets the

requirements of many pulsed beam inspections in industrial and medical applications.

In addition to the above applications, some long-chain alkylamine series of hybrid perovskite structures, such as $(C_nH_{2n+1}NH_3)_2 MX_4$ ($n = 12, 14, 16$), due to their unique double layer similar to bio phospholipids Structure, there is a phase change process in the low temperature region, the solid structure can change from directed order to disorder, and the latent heat of phase change is large. It can be predicted that they have certain application prospects in low temperature energy storage materia.in addition, due to transition metals.^[46,047] The orbital characteristics of the electron spins, the magnetic properties of the hybrid perovskite are very good, and the divalent cations of the transition metal are generally stable. Therefore, transition metal-based hybrid perovskites have also been extensively studied in terms of two-dimensional magnetic properties and diamagnetic properties.

1.4. The purpose and significance of the research

The organic/inorganic hybrid perovskite material has a special super-element quantum well structure. By selecting suitable organic

molecules and inorganic molecules, the optical band properties, carrier mobility and other photoelectric properties of the material can be controlled in a wide range. Organic/inorganic hybrid perovskite materials combine all the advantages of organic and inorganic materials to make up for their respective deficiencies, structural and performance with flexible design, showing their presence in flat panel displays, nonlinear optics, field effect transistors wide application prospects for optoelectronic devices such as light-emitting diodes and solar cells.

Although the preparation technology of organic/inorganic hybrid perovskite materials has been developed, the research on basic structure and properties is also very extensive, but it is basically limited to the hybrid perovskite of single-layer inorganic layer, by changing inorganic The number of layers (m) or the length of the organic chain (n) to regulate the energy level and photoelectric properties of the perovskite structure is relatively small, and its application for excellent structural, optical and optoelectronic properties is adjustable. Optoelectronic devices with flexible, stable and efficient structural design still play an important role in the research of organic/inorganic hybrid perovskite materials. ^[48, 49]

Based on the existing work, the excellent film-forming properties of

hybrid perovskite materials were used to synthesize the different organic components of lead iodide series and the hybrid perovskite materials and films with different inorganic layers. Analyze the energy level structure, optical properties, etc. of the material through structural and performance characterization tests; form a multilayer heterostructure organic/inorganic hybrid perovskite with TiO_2 , copper phthalocyanine (CuPc) and other inorganic or organic semiconductors Guide or photovoltaic devices, and improve device performance through energy level regulation and parameter optimization, and further analyze its energy transfer (photoelectric transfer) mechanism. These studies have improved the research on the controllability and design of hybrid perovskites. It is of great significance in the development of high-performance organic/inorganic photovoltaic functional materials and optoelectronic devices, and in reducing production costs.

2. Background: Synthesis and Characterization of Organic/Inorganic Hybrid Perovskite Materials Based on Lead Iodide

2.1. Introduction

Hybrid perovskites of the Group IVA metal halides have excellent semiconductor properties, and their intense photoluminescence properties and high carrier mobility have attracted extensive attention and research. For organic/inorganic hybrid perovskite materials, the choice of inorganic components can affect the structure and physical properties of the material. The choice of organic components can also control the dimensionality of the inorganic layer and affect the crystal orientation of the inorganic framework structure. Ultimately affecting the physical properties of the hybrid material, in addition, the organic component can provide good self-assembly and processing properties of the material and can also regulate the performance.

In this chapter, we selected several linear alkylamines of different alkyl chain lengths and aromatic amines containing monocyclic rings as organic components to make PbI_2 which is stable in air as an inorganic

component, and to prepare different ones.^[50-53] An organic composition of lead iodide-based hybrid perovskite crystal material (wherein the organic component is a linear alkyl ammonium cation $C_nH_{2n+1}NH_3^+$ ($n=4, 8, 12$) or a phenethyl ammonium salt cation $C_6H_5C_2H_4NH_3^+$), and then passed The corresponding hybrid perovskite film was prepared by spin coating. The effects of organic composition on the crystal structure and photoelectric properties of hybrid perovskite materials were systematically studied by means of ray diffraction, ultraviolet-visible absorption spectroscopy, fluorescence spectroscopy and other experimental methods.^[54-56] This will further study the synthesis of perovskite materials. The optimization of its performance is extremely important.

2.2. Experimental part

2.2.1. Chemical reagents

Table 2.1 The reagent list

| Number | Reagent | Specification |
|--------|--|---------------|
| 01 | CH ₃ NH ₂ | AR |
| 02 | C ₄ H ₉ NH ₂ | AR |
| 03 | C ₈ H ₁₇ NH ₂ | AR |
| 04 | C ₁₂ H ₂₅ NH ₂ | AR |
| 05 | C ₆ H ₅ C ₂ H ₄ N ₂ | AR |
| 06 | HI | AR |
| 07 | PbI ₂ | AR |
| 08 | C ₂ H ₅ OH | AR |
| 09 | C ₃ H ₇ NO | AR |
| 10 | C ₃ H ₆ O | AR |
| 11 | H ₂ SO ₄ | AR |
| 12 | H ₂ O ₂ | AR |

2.2.2. Preparation of organic amine salts

C₄H₉NH₃I: Under the condition of ice water solubility, n-butylamine and ethanol are mixed into a mixed solution, magnetically stirred under

the protection of chlorine gas, and an excessive amount of concentrated hydroiodic acid is slowly added thereto. After the reaction is completed, the crude product is obtained by vacuum distillation under reduced pressure. (with yellow impurities), rinsed with diethyl ether to give a white $C_4H_9NH_3I$ crystal, which was then dried in vacuo at $70\text{ }^\circ\text{C}$ for 12 h. The preparation method of other organic salt ($C_8H_{17}NH_3I$, $C_{12}H_{25}NH_3I$, and $C_6H_5C_2H_4NH_3PbI$) is the same as $C_4H_9NH_3I$.

2.2.3. Preparation of organic/inorganic hybrid calcium ore materials

2.2.3.1. Preparation of hybrid calcium mineral crystal material

$(C_4H_9NH_3)_2PbI_4$ crystal: dissolve the $(C_4H_9NH_3)_2PbI_4$ in a concentrated hydroiodic acid solution with a molar ratio of 1:2, place it in a $75\text{ }^\circ\text{C}$ water bath, react for 1 hour, remove, slowly cool, and then filter, ether. The rinsing was repeated several times, and then recrystallized twice with absolute ethanol to obtain a golden yellow metallic flaky crystal, which was dried in a vacuum oven at $70\text{ }^\circ\text{C}$ and stored in a desiccator. A series of hybrid calcium mineral structure crystal materials such as $(C_8H_{17}NH_3)_2PbI_4$, $(C_{12}H_{25}NH_3)_2PbI_4$ and $(C_6H_5C_2H_4NH_3)_2PbI_4$, etc.

are prepared as above.

2.2.3.2. Preparation of hybrid calcium ore film

(a) Cleaning and hydrophilic pretreatment of quartz plates

The quartz plate was cleaned with water, and then ultrasonically cleaned in pure solvent of isopropanol, acetone, toluene, acetone and ethanol for 2 minutes, then ultrasonically shaken for 2 minutes in deionized water, repeated two or three times until it is washed.

Prepare a mixed solution of concentrated sulfuric acid and hydrogen peroxide in a volume ratio of 3:1. Carefully put the cleaned quartz plate into the mixed solution (be careful to prevent the quartz plate from laminating in the solution), and heat the mixture to maintain the temperature of the mixture at 75 °C.

(b) Preparation of film

($C_4H_9NH_3$)₂PbI₄ film: $C_4H_9NH_3I$, PbI_2 is formulated into a 10 mg/mL DMF solution at a stoichiometric ratio of 1:2, using a hydrophilic ally treated quartz glass as a substrate, and a tabletop homemaker (KW-4A type) at 2000 mm. The coating was spin-coated at a rate of 30 t and dried

in a vacuum oven at 70 ° C for 30 min to obtain a yellow film. The $(C_8H_{17}NH_3)_2PbI_4$, $(C_{12}H_{25}NH_3)_2PbI_4$ and $(C_6H_5C_2H_4NH_3)_2PbI_4$ films were prepared in the same manner as $(C_4H_9NH_3)_2PbI_4$.

2.2.4. Characterization means

2.2.4.1. X-ray diffraction (XRD)

The experiment used X-ray shot, model Bruker D8 Discover, $Cu K\alpha$, $\lambda = 0.154406$ nm powder or film samples.

2.2.4.2. UV-visible light absorption (UV-Vis)

Ultraviolet absorption spectrometer, model Hatchet-3900. The sample is a film spin-coated on a quartz substrate.

2.2.4.3. Fluorescence spectrum (PL)

A fluorescence analyzer, model Hitachi F-7000, was used to sample the film on the quartz substrate.

2.3. Spectroscopic measurement

2.3.1. Analysis of the structure of hybrid perovskite materials

The Fig. 2.1 A, B, C, and D show XRD diffraction patterns of four hybrid perovskite crystal materials of $(\text{C}_4\text{H}_9\text{NH}_3)_2\text{PbI}_4$, $(\text{C}_8\text{H}_{17}\text{NH}_3)_2\text{PbI}_4$, $(\text{C}_{12}\text{H}_{25}\text{NH}_3)_2\text{PbI}_4$ and $(\text{C}_6\text{H}_5\text{C}_2\text{H}_4\text{NH}_3)_2\text{PbI}_4$, respectively. As shown in Figures A, B, C, and D, except for the diffraction peaks of the $(00l; l = 2, 4, 6, 8\dots)$ series which are perpendicular to the c-axis, there is substantially no diffraction in other directions peak, which indicates that the purity of the product is high, the periodicity is good, and its structure has obvious orientation in the c-axis direction, and has a very regular layered structure. In addition, the intensity of the diffraction peak of the film is significantly larger than that of the powder peak strength, which indicates that the film is more favorable to the crystallization and orientation of the hybrid perovskite material than the powder.

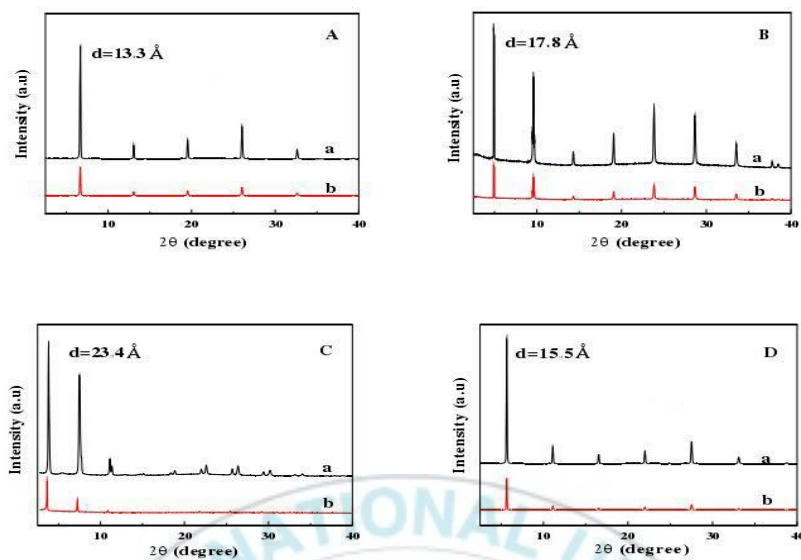


Fig. 2.1 Powder X-ray diffraction patterns of (A) $(\text{C}_4\text{H}_9\text{NH}_3)_2\text{PbI}_4$, (B) $(\text{C}_8\text{H}_{17}\text{NH}_3)_2\text{PbI}_4$, (C) $(\text{C}_{12}\text{H}_{25}\text{NH}_3)_2\text{PbI}_4$ and (D) $(\text{C}_6\text{H}_5\text{C}_2\text{H}_4\text{NH}_3)_2\text{PbI}_4$ powder and thin films, respectively.

Since the system hybridized perovskite materials have a two-dimensional layered orientation, their layer spacing (d) can be calculated using the Bragg formula:

$$2d \sin \theta = n\lambda$$

This experiment uses monochromatic $\text{Cu K}\alpha$ radiation, λ is equal to 1.5406 \AA , and n is the diffraction order (e.g. first-order diffraction peak, $n=1$). From the first-order diffraction peaks on the (002) plane of XRD

($2\theta=6.701^\circ, 4.941^\circ, 3.838^\circ, 5.670^\circ$), $(C_4H_9NH_3)_2PbI_4$, $(C_8H_{17}NH_3)_2PbI_4$, $(C_{12}H_{25}NH_3)_2PbI_4$ and $(C_6H_5C_2H_4NH_3)_2PbI_4$ can be calculated. The layer spacing d values are 11.5 Å, 17.8 Å, 23.4 Å and 15.5 Å, respectively. Their corresponding unit cell parameters c are 23.0 Å, 35.7 Å, 46.8 Å and 31 Å, respectively.

NV. Venkataraman et al. found that in the $(C_4H_9NH_3)_2PbI_4$ series of long-chain alkylamine hybrid perovskite crystals, the number of carbon atoms increases, the structure of the inorganic layer remains unchanged, and the length of the organic layer. The alkylamines are arranged in a double layer and adopt an all-trans conformation, and calculated by XRD, the interlayer spacing is increased by 1.36 Å for each additional methylene group. It can be inferred that there is a tilt angle of 57° between the organic chain and the inorganic layer.

When the number of carbon atoms of the linear organic amine increases ($C_4 \rightarrow C_8 \rightarrow C_{12}$), the alkyl segment becomes longer, and the interlayer spacing of the hybrid perovskite increases (11.5 Å \rightarrow 17.8 Å \rightarrow 23.4 Å). This is equivalent to increasing the interlayer spacing by 6.3 Å and 5.6 Å for each additional methylene group. It is thus known that for every 4 methylene groups added, the interlayer spacing increases by an

average of 5.9 Å, which is equivalent to an increase in the interlayer spacing per methylene group. 1.48Å. If the long-chain alkylamine is perpendicular to the inorganic layer, the layer spacing of the hybrid perovskite crystals of the double-layer organic chain will increase by 2.5 Å for each additional methylene unit, and the alkyl chain is not perpendicular to the inorganic layer, assuming that the tilt angle of the alkyl chain and the inorganic layer is θ , then the layer spacing $d = A + 2.5 \cos \theta = A + 1.48$. Based on this, the alkyl chain layer and the inorganic layer can be deduced. The inclination angle θ between them is about 54°, which is substantially equivalent to the above theoretical value. Therefore, it can be seen that the organic layers of the $(C_nH_{2n+1}NH_3)_2PbI_4$ series of perovskite structures are arranged at a certain oblique angle: while the inorganic framework $[PbI_6]^{4-}$ plays an important role in maintaining the orientation and regularity of the structure, the length of the organic chain is The effect of this two-dimensional inorganic layered structure is small.

[57, 58]

2.3.2. UV-Vis absorption spectroscopy analysis of hybrid perovskite films

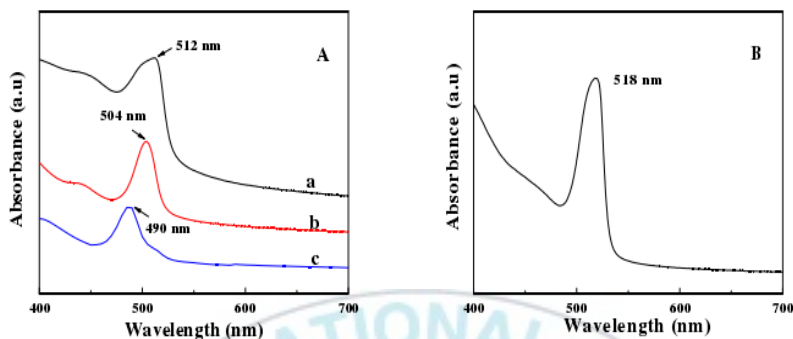


Fig. 2.2 The UV-Vis absorption spectra of (A) $(C_4H_9NH_3)_2PbI_4$ (a), $(C_8H_{17}NH_3)_2PbI_4$ (b), and $(C_{12}H_{25}NH_3)_2PbI_4$ (c), (B) $(C_6H_5C_2H_4NH_3)_2PbI_4$ thin films, respectively.

$(C_8H_{17}NH_3)_2PbI_4$ (b), and $(C_{12}H_{25}NH_3)_2PbI_4$ (c) hybrid perovskite film.

The absorption peaks of the materials are located at 512 nm, 504 nm and 490 nm; Figure 2.2B shows the absorption spectrum of the $(C_6H_5C_2H_4NH_3)_2PbI_4$ hybrid perovskite film with an absorption peak at 518 nm. The absorption peaks of these PbI_4^{2-} -based hybrid perovskite films are typical exciton absorption peaks. In the two-dimensional layered hybrid perovskite, due to the synergistic effect of the quantum

confinement effect and the dielectric confinement effect, the hybrid perovskite material has a large exciton binding energy and is prone to exciton absorption. Meanwhile, since the organic molecules $C_nH_{2n+1}NH_2$ and $C_6H_5C_2H_4NH_2$ are transparent in the visible light region, absorption can be considered to be caused by exciton in the $[PbI_6]^{4-}$ inorganic layer. The valence band of the $[PbI_6]^{4-}$ inorganic layer is formed by the hybridization of $Pb^{2+}(6s)$ orbital and $I(5p)$ orbital, and the conduction band is composed of $Pb(6p)$. When the energy of absorbed light $h\nu \geq E_g$ (E_g is the forbidden band width), electrons from the price band to the conduction belt.^[59]

Organic/inorganic hybrid perovskite materials have different absorption peak positions due to differences in optical band gaps. As the forbidden band width of the material increases in turn, the energy required for the electrons to transition from the valence band guide band increases, and the absorption peak of the material undergoes a blue shift (moving in the short-wave direction). As shown in Figure 2.2A, the absorption peak positions of a, b, and c are blue-shifted (512 nm \rightarrow 504 nm \rightarrow 490 nm), indicating the optical inhibition of hybrid perovskite $(C_4H_9NH_3)_2PbI_4$,

$(C_8H_{17}NH_3)_2PbI_4$, and $(C_{12}H_{25}NH_3)_2PbI_4$. The bands are added one

after the other. The absorption peak of $(\text{C}_6\text{H}_5\text{C}_2\text{H}_4\text{NH}_3)_2\text{PbI}_4$ is at the maximum wavelength position compared with the other three hybrid perovskites (**Fig. 2.2B**), indicating that the optical forbidden band is the smallest, which may be due to the introduction of the benzene ring and the conjugation effect of the large π bond. Electrons have better transport properties, thus reducing the energy required for electronic transitions. Adding functional organic molecules, especially organic substances with chromophores, can control the band structure and optical properties of hybrid perovskite materials.

2.3.3. Fluorescence (PL) spectral analysis of hybrid perovskite films

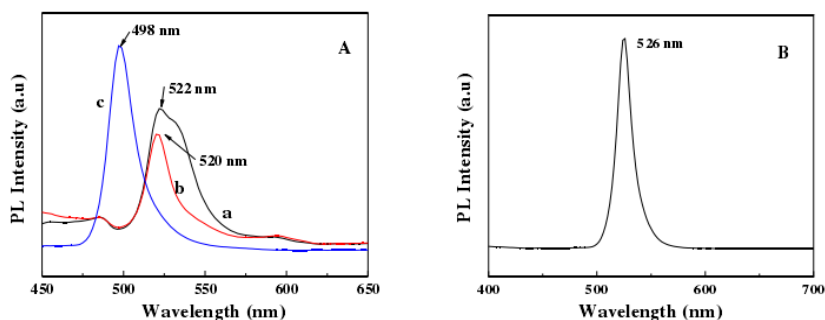


Fig. 2.3 The PL (A) $(\text{C}_4\text{H}_9\text{NH}_3)_2\text{PbI}_4$ (a), $(\text{C}_8\text{H}_{17}\text{NH}_3)_2\text{PbI}_4$ (b), and

(C₁₂H₂₅NH₃)₂PbI₄ (c), (B) (C₆H₅C₂H₄NH₃)₂PbI₄ thin films at room temperature, respectively.

In Fig. 2.3A, a, b and c are the photoluminescence spectra of (C₄H₉NH₃)₂PbI₄, (C₈H₁₇NH₃)₂PbI₄, and (C₁₂H₂₅NH₃)₂PbI₄ films at room temperature, respectively. The peak shape is sharp and the emission peaks are 522 nm (a) and 520 nm (b) and 498 nm (c); Fig. 2.3B shows the photoluminescence of (C₆H₅C₂H₄NH₃)₂PbI₄ film at room temperature with an emission peak of 526 nm and a sharper peak shape than a linear amine salt hybrid perovskite. And the half width is small, which indicates that the fluorescent color of (C₆H₅C₂H₄NH₃)₂PbI₄ is higher. Their excitation wavelengths are all 370 nm. As can be seen from the figure, these four hybrid perovskite materials have sharp emission peaks, peak intensity are quite large, and Stokes between the exciton absorption peak and the fluorescence emission peak. The displacement is relatively small, which means that the fluorescence emission peak comes from the free excitons rather than the self-trapped exciton surface. At room temperature, the yellow-green (green) emission of such hybrid perovskites can be observed with the naked eye, and the color High purity.^[60]

Relative to PbI_2 , organic molecules ($\text{C}_n\text{H}_{2n+1}\text{NH}_2$ and $\text{C}_6\text{H}_5\text{C}_2\text{H}_4\text{NH}_2$) have larger band gaps (the difference between HOMO and LUMO), and the forbidden band of PbI_2 will completely fall in the HOMO-LUMO band of organic molecules, forming type I. Quantum well structure (see 1.2.2) electrons and holes will be confined in the same layer ($[\text{PbI}_6]^{4-}$ layers), excitons are prone to radiation recombination and emit photons, resulting in photoluminescence.

Since the organic molecules ($\text{C}_n\text{H}_{2n+1}\text{NH}_2$ and $\text{C}_6\text{H}_5\text{C}_2\text{H}_4\text{NH}_2$) are optically inert, the strong photoluminescence properties are derived from the exciton radiation attenuation of the inorganic layer. It is generally believed that the strong luminescence of such two-dimensional layered hybrid perovskite materials at room temperature is caused by their large exciton binding energy. Ordinary undoped inorganic semiconductor materials have less exciton binding energy (tens of mega-electron volts), and the exciton binding energy of PbI_2 is only 30 meV, and the exciton binding energy of the composite hybrid perovskite is very large, usually a few hundred millielectron volts, is much larger than KT at room temperature (KT is about 26 meV at 300K). Such hybrid perovskite materials have large exciton binding energy, which is generally considered

to be the result of both the dielectric confinement effect and the two-dimensional quantum confinement effect. In addition, the benzene ring is compared with the linear alkyl group. The addition enhances the energy (electron) transfer between the organic layer and the inorganic layer, and thus has more excellent photoluminescence properties.

Through the above experimental results and analysis, it is known that the type of hybrid quantum perovskite quantum well is affected by the relative energy band positions of inorganic components and organic components, which will affect the luminescence properties of the materials; more importantly, The synergistic effect of the electric confinement effect and the two-dimensional quantum confinement effect, the two-dimensional layered hybrid perovskite material has large exciton binding energy, which is a necessary condition for photoluminescence. Therefore, we can adjust the luminescence properties of hybrid perovskites by varying organic components (chain length, choice of functional groups) and inorganic components (metal cations, anion selection). Due to its large exciton binding energy, strong fluorescence and good color purity, hybrid perovskite materials have unlimited application potential in luminescent materials and LED display fields.

3. Sample preparation and Discussions

3.1. Sample preparation

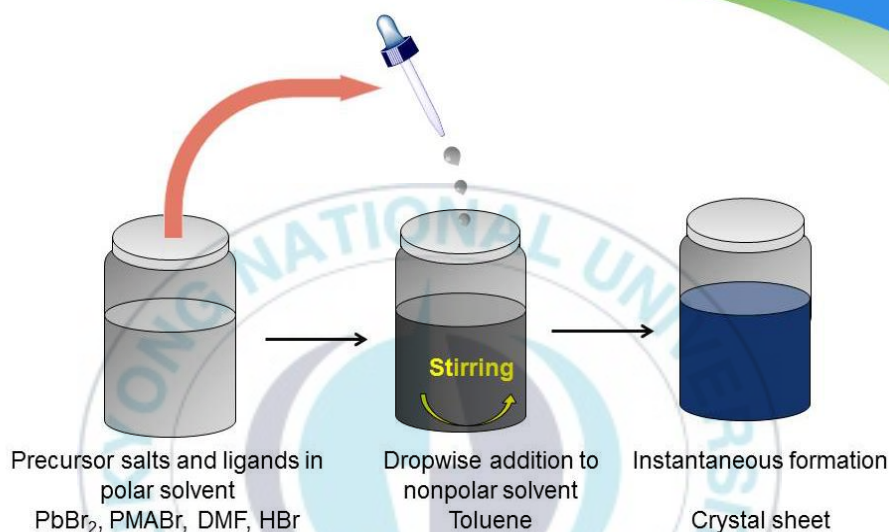


Fig. 3.1 Synthesis process of the $(\text{PMA})_2\text{PbBr}_4$.

As shown in the **Fig. 3.1**, the $(\text{PMA})_2\text{PbCl}_2\text{Br}_2$ precursor solution was obtained by dissolving stoichiometric of PMABr, HBr, and PbBr_2 in 1ml of N,N-dimethylformamide (DMF) with continuous stirring at 90 °C. Then, the precursor solution was drop wise added to 10 ml of toluene. The $(\text{PMA})_2\text{PbBr}_4$ solution was quenched and the crystal is obtained. After being filtered and washed with acetone three times, the white powder was dried at 60 °C in vacuum for 10 h.

3.2. Results and discussions

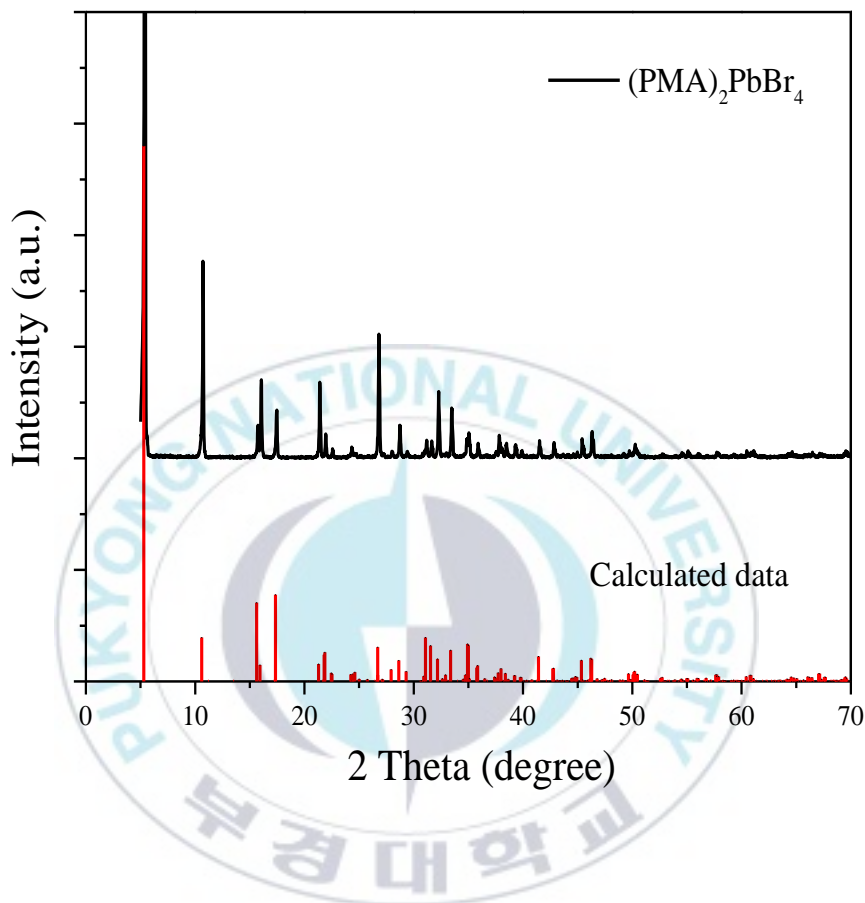


Fig. 3.2 XRD data of the $(\text{PMA})_2\text{PbBr}_4$ perovskite film on a quartz substrate

Fig. 3.2 shows the XRD patterns of the $(\text{PMA})_2\text{PbBr}_4$ perovskite film on a quartz substrate along with the calculated standard PDF card. Diffraction peaks of all the samples are well indexed to the structural results for $(\text{PMA})_2\text{PbBr}_4$ single crystal. No traces of impurities were

detected suggests that $(\text{PMA})_2\text{PbBr}_4$ perovskite film has been prepared successfully.

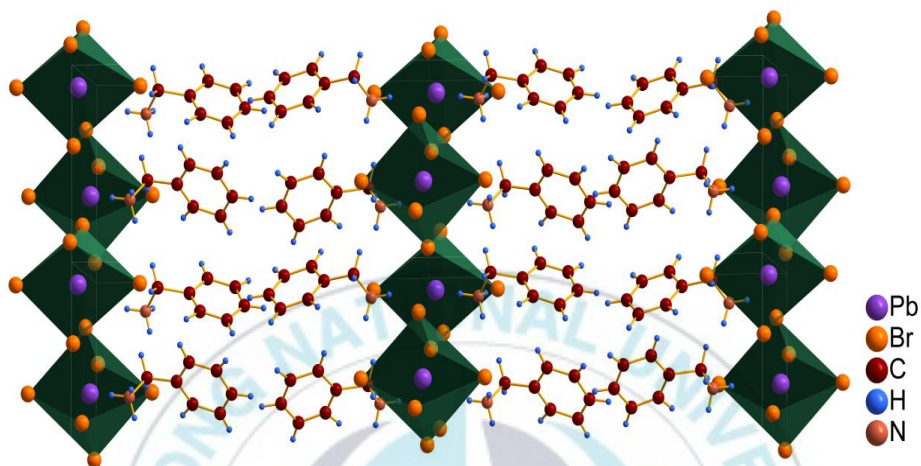


Fig. 3.3 Schematic structure of the typical 2D organo-lead halide perovskite $(\text{PMA})_2\text{PbBr}_4$

Fig.3.2 shows the XRD patterns of the powder sample, all the experimental peaks are corresponding to the simulated data. It means that our sample has pure phase. **Fig.3.3** shows the schematic structure of layered perovskite. Alternating layers of organic amine and inorganic semiconductor are formed in these compounds in a self-organized manner. This structure exhibits unique optical properties due to quantum confinement of the Wannier excitons in the inorganic layers.

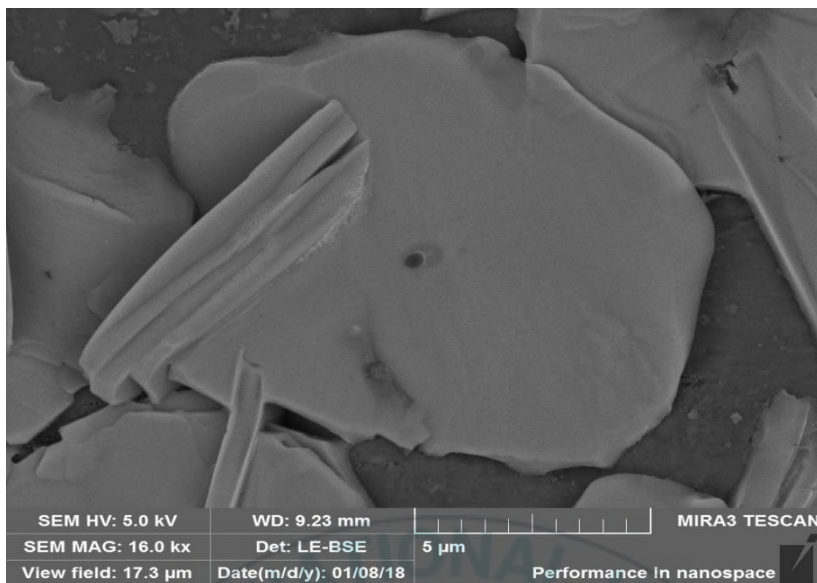


Fig.3.4 SEM images of the $(\text{PMA})_2\text{PbBr}_4$.

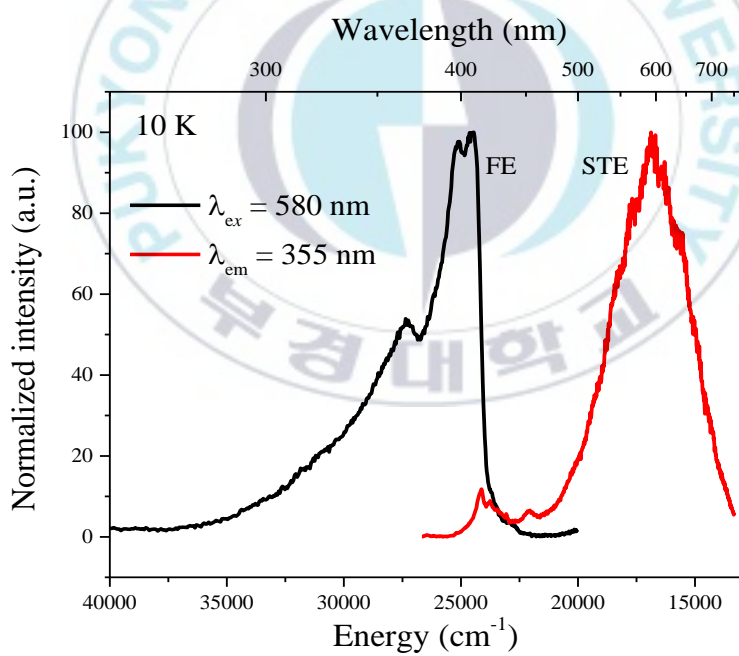
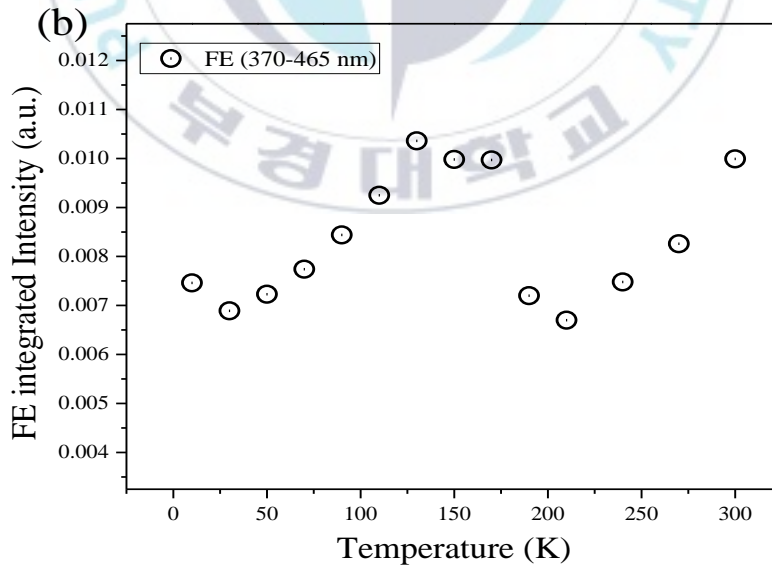
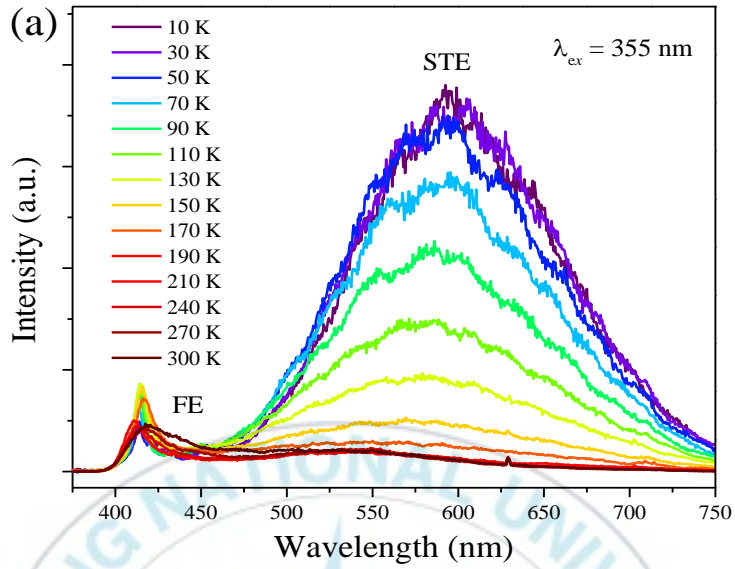


Fig.3.5 Normalized PL and PLE spectra of the $(\text{PMA})_2\text{PbBr}_4$.

The 10 K photoluminescence excitation (PLE) and emission (PL) spectra of the $(\text{PMA})_2\text{PbBr}_4$ perovskite are depicted in **Fig.3.5**. The excitation spectrum is similar to other isostructural 2D perovskites with band absorption (around 300 nm) and a sharp peak absorption (around 375 nm).^[67] The absorption band can be assigned to the electronic transitions of the Pb (6s) orbital hybridized with the Br (4p) and Cl (3p) orbital states in the inorganic layers, and the narrow sharp peak absorption can be attributed to the excitonic absorption caused by the quantum and dielectric confinement effects.^[62] Under the 355 nm laser excitation, a broad structureless band photoluminescence (PL) range of 365 - 700 nm with a shoulder located at around 425 nm can be detected by the time-integrated emission technique. According to the reference, we assigned the band located at around 425 nm as free exciton emission (FE). The broadband with a large Stokes shift indicates strong electron-lattice coupling and could be assigned as self-trapped excitons (STEs) in a deformable lattice.^[63]



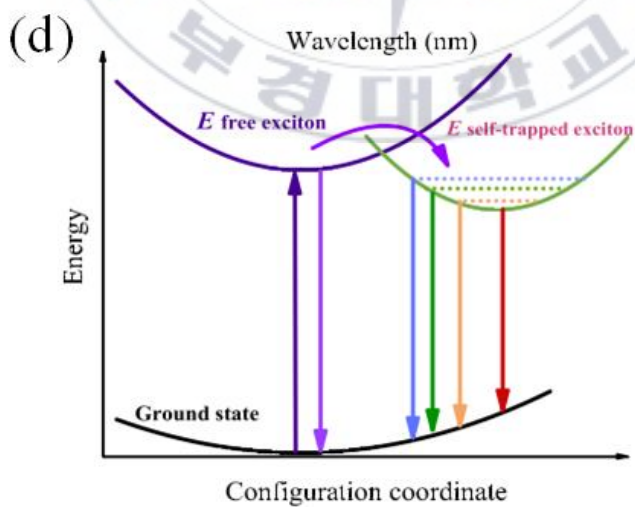
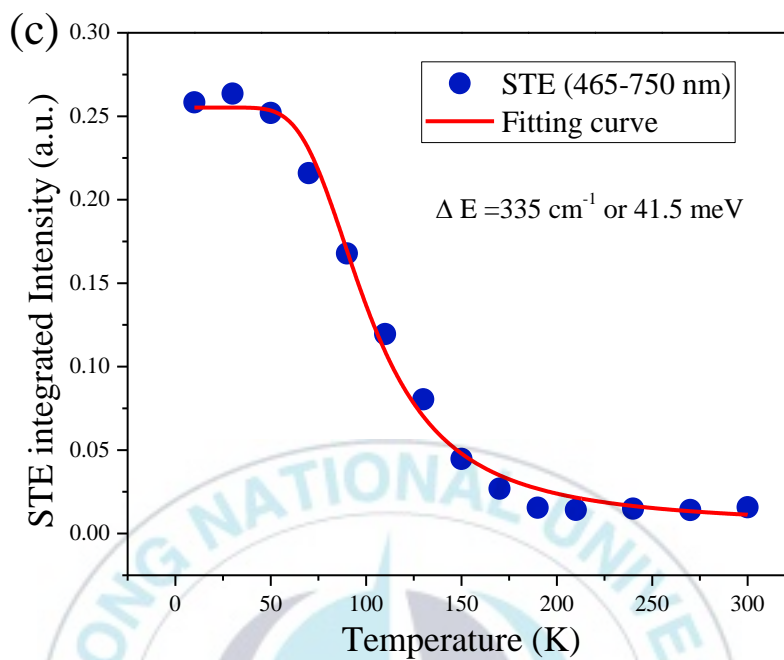


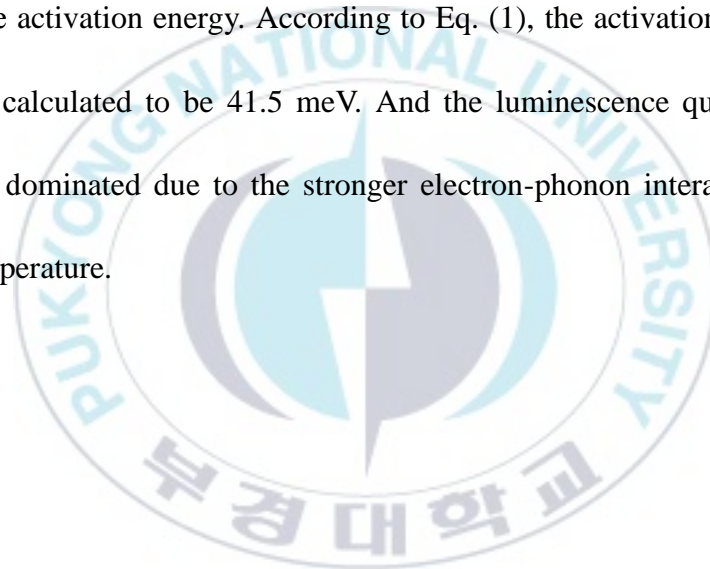
Fig.3.6 (a) Temperature dependent emission spectra of the $(\text{PMA})_2\text{PbBr}_4$ thin film; (b) Calculated temperature dependent integrated FE emission intensities of $(\text{PMA})_2\text{PbBr}_4$ thin film; (c) Calculated temperature dependent integrated STE emission intensities of $(\text{PMA})_2\text{PbBr}_4$ thin film fitted into the referred equation. (d) Configuration coordinate diagram demonstrating the coexistence of free and self-trapping excitons in the 2D perovskite frameworks.

Fig. 3.6 shows the temperature dependent PL spectra, calculated temperature dependent integrated FE and STE emission intensities in the range of 10 to 300 K, and the possible mechanism responsible for the interaction between the FE and STE emissions in $(\text{PMA})_2\text{PbBr}_4$. With the increasing temperature, the excitons created from the FE states have more possibility to relax into the STE states (the curved purple arrow represents the relaxation process in **Fig. 3.6(d)**); the integrated intensity of FE shows a complex thermal evolution. The FE intensity firstly increased from 10 to 150 K, due to energy back transfer, and then decreased due to thermal quenching, the PL enhancement between 200 and 300 K is due to spectra thermal brooding. The broad STE emission

with large stokes shift could be fitted by a simple thermal activation model.

$$I_T = I_0 \cdot \left[1 + c \cdot \exp\left(-\frac{\Delta E}{kT}\right) \right]^{-1} \quad (1)$$

where I_0 is the initial emission intensity, I_T is the intensity at different temperatures, c is a rate constant for the thermally activated escape, and ΔE is the activation energy. According to Eq. (1), the activation energy ΔE was calculated to be 41.5 meV. And the luminescence quenching effect is dominated due to the stronger electron-phonon interaction at high temperature.



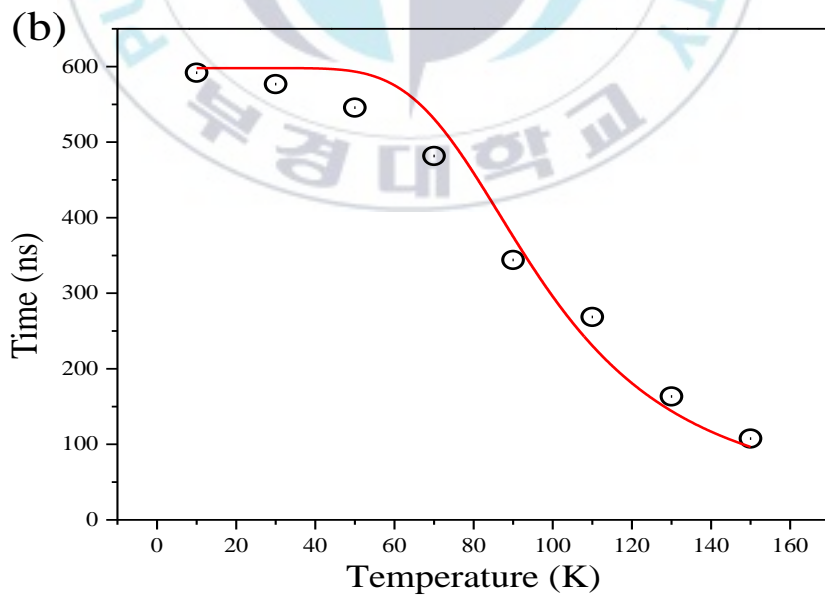
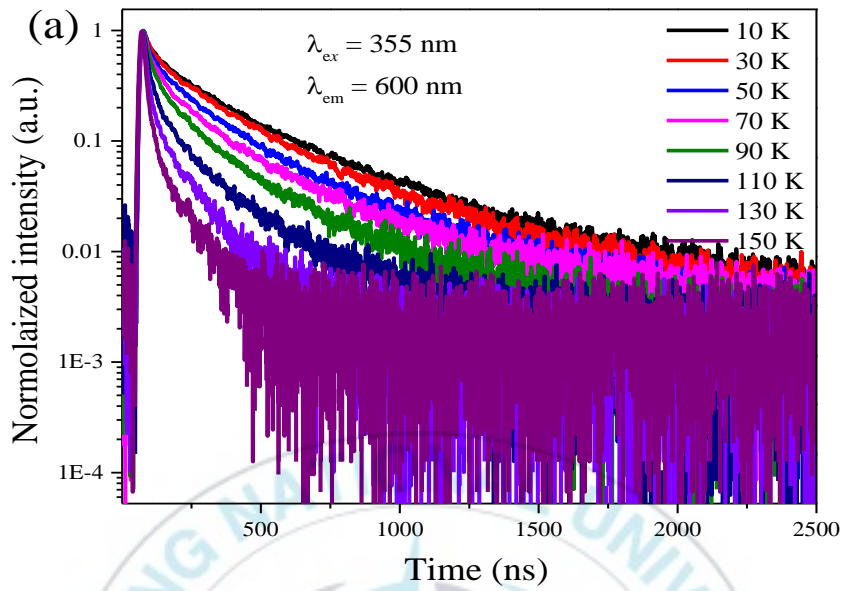


Fig. 3.7 (a) Temperature dependent decay curves of the (PMA)₂PbBr₄ thin film; **(b)** Calculated temperature dependent integrated STE lifetimes of (PMA)₂PbBr₄ thin film.

To better understand the thermal quenching phenomenon for (PMA)₂PbBr₄ thin film and confirm the influence of temperature on the energy transfer rate, the fluorescence decay curves for (PMA)₂PbBr₄ thin film were measured at 355 nm excitation by monitoring the emission at 600 nm in the temperatures between 10 and 150 K, and the maximum-intensity-normalized decay curves are shown in **Fig. 3.7 (a)**. It is obviously seen that the fluorescence decay curves are non-exponential and these fluorescence decay curves display non-exponential curves can be fitted to the effective lifetimes defined as the following:^[64,65]

$$\tau_{\text{average}} = \frac{\int tI(t)dt}{\int I(t)dt} \quad (2)$$

where I(t) represents the luminescence intensity at a time t after the cutoff of the excitation light. The luminescence lifetimes of the (PMA)₂PbBr₄ thin film calculated as a function of temperature and displayed in **Fig. 3.7 (b)**. Generally, with the increase of temperature, the probabilities of multiphonon relaxation and energy transfer for quenching the emitting

levels may be enhanced, which are responsible for the decrease of luminescence intensity. As calculated, the lifetimes shorten monotonically from 600 ns (10 K) to 150 ns (150 K).

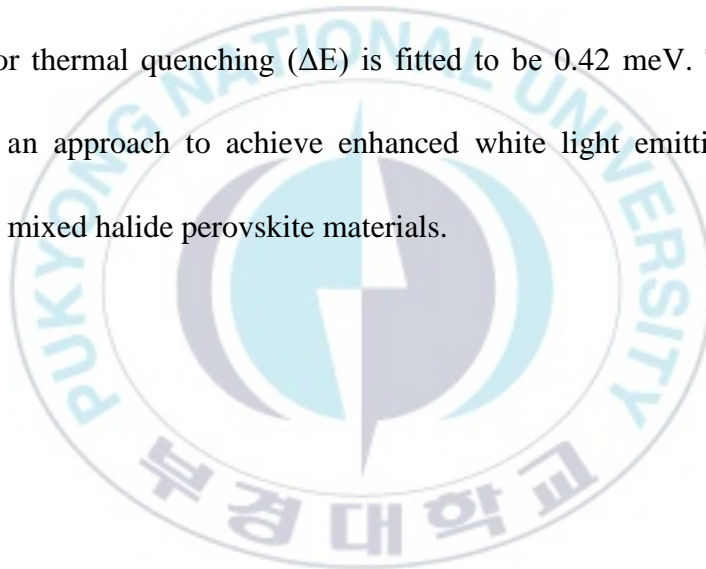
The thermal activation energy (ΔE) for the thermal quenching of the $(\text{PMA})_2\text{PbBr}_4$ thin film was also determined by measuring the temperature dependence of emission lifetime (fitting curve in **Fig. 3.7 (b)**).^[66,67] The temperature dependence of the emission lifetime is described by the equation as follows:

$$\tau(T) = \frac{\tau_r}{1 + [\tau_r / \tau_{nr}] \exp(-\Delta E / kT)} \quad (3)$$

where τ_r and τ_{nr} are radiative and non-radiative decay times, and k is the Boltzmann constant ($8.6299 \cdot 10^{-5}$ eV). The thermal activation energy for thermal quenching (ΔE) is fitted to be 42.1 meV. This is in agreement with the calculated value calculated on decay lifetimes according to Eq. (1).

4. Conclusions

In summary, we reported a bluish-white-light emitting diode using 2D mixed halide perovskite $(\text{PMA})_2\text{PbBr}_4$. Temperature dependent emission spectra and decay curves reveal that the white emission band consists of free exciton and self-trapped exciton transition. Based on the temperature dependent emission spectra and decay curves, the thermal activation energy for thermal quenching (ΔE) is fitted to be 0.42 meV. This work provides an approach to achieve enhanced white light emitting diodes using 2D mixed halide perovskite materials.



Acknowledgements

Foremost, I would like to express my gratitude to my supervisor, professor Hyo JinSeo, for his continuous support, patience, encouragement and immense knowledge that contributed to the completion of thesis. His guidance has helped me a lot during the two years of research and living in South Korea. I would like to extend my sincere thanks to Dr. Peiqing Cai. Thanks to his instructive guidance and comprehensive education during the two years' schooling.

I would like to express my appreciation to all of my warmhearted lab-mates, Lin Qin, Cuili Chen, JingWang, Shala Bi, and Zutao Fan, who gave me their kindly help both in my learning and living. I also would like to express my gratitude to my roommate Qian Song, who gave me a lot of help during my life in Korea.

Last but not least, I am grateful to my parents and other relatives, thank you for your support and encouragement during these years.

References

- [1] D.B. Mitzi, M.T. Prikas, K. Chondroudis, Thin film deposition of organic-inorganic hybrid Materials using a single source vapor deposition [J]. Chem. Mater., 119 (1999) 542-544.
- [2] P. Cai, X. Wang, H. Seo, et al. Bluish-white-light-emitting diodes based on two-dimensional lead halide perovskite $(\text{C}_6\text{H}_5\text{C}_2\text{H}_4\text{NH}_3)_2\text{PbCl}_2\text{Br}_2$. Appl. Phys Lett, 112 (2018) 153901.
- [3] Z. Cheng, J. Lin, Layered organic-inorganic hybrid perovskites: structure, optical properties, lm preparation, patterning and templating engineering [J]. Cryst. Eng. Comm., 12 (2010) 2646-2662.
- [4] Y. Zheng, Research on Photoelectric Functional Materials of Organic/Inorganic Hybrid Calcium Mineral Structure [D]. Zhejiang University, 2007.
- [5] I.B. Koutselas, D.B. Mitzi, G.C. Papavassiliou, et al. Optical and related properties of natural One-dimensional semiconductors based on PbI and SnI units [J]. Synthetic Metals, 86 (1997) 2171-2172.
- [6] D.B. Mitzi, L.L. Kosbar, C.E. Murray, et al. High-mobility ultrathin semiconducting films Prepared by spin coating [J]. Nature, 428 (2004) 299-303.
- [7] B. Kundys, A. Lappas, M. Viret, et al. Multiferroicity and hydrogen-bond ordering in $(\text{C}_2\text{HSNH}_3)_2\text{CuCl}_4$ featuring dominant ferromagnetic interactions [J]. Phys. Rev. B, 81 (2010) 224434.
- [8] K. Lee, C. Lee, Magnetic resonance study of the two-dimensional spin diffusion in the Heisenberg paramagnet $(\text{C}_{18}\text{H}_{37}\text{NH}_3)_2\text{MnCl}_4$ [J]. Solid

State Communications, 126 (2003) 343-346.

[9] T. Shihara, J. Takahashi, T. Goto, et al. Optical properties due to electronic transitions in Two-dimensional semiconductors $(\text{CH}_2\text{NH}_3)_2\text{PbI}_4$. Phys. Rev. B, 42 (1990) 11099-11111.

[10] J. Calabrese, N.L. Jones, R.L. Harlow, Preparation and characterization of layered lead halide Compound [J]. J. Am. Chem. Soc., 113 (1991) 2328-2330.

[11] D.B. Mitzi, S. Wang, C.A. Feild, et al. Conducting layered organic-inorganic halides containing <110>-oriented perovskite sheet [J]. Science, 267 (1995) 1473-1476.

[12] D.B. Mitzi, C.A. Feild, Harrison WTA, et al. Conducting tin halides with a layered Organic-based perovskite structure [J]. Nature, 369 (1994) 467-469.

[13] D.B. Mitzi, Synthesis, structure and properties of organic-inorganic perovskites and related materials [J]. Chem. Inform., 30 (1999) 1 121.

[14] D.B. Mitzi, K. Chondroudou, C.R. Kagan, Organic-inorganic electronics [J]. IBM J. Res.&D., 45 (2001) 29-32.

[15] K. Pradeesh, J.J. Baumberg, G.V. Prakash, In situ intercalation strategies for device-quality Hybrid inorganic-organic self-assembled quantum wells [J]. Appl. Phys. Lett., 95 (2009) 033309

[16] Y. Li, G. Zheng, C. Lin, et al. New organic-inorganic perovskite materials with different optical properties modulated by different inorganic sheets [J]. Cryst Growth Des, 8 (2008) 1990-1996.

[17] T. Ishihara, J. Takahashi, T. Goto, Optical properties due to electronic transitions in Two-dimensional semiconductors $(\text{CH}_2\text{NH}_3)\text{ZPbI}_4$ [J]. Phys.

Rev. B, 42 (1900) 11099.

[18] J. Ku, Y. Lansac, Y. Jang, Time-dependent density functional theory study on benzene diazole-based low-band-gap fused-ring copolymers for organic solar cell applications. *J. Phys. Chem. C* ;11 (2011) 18372-18377.

[19] V.K. Komar, V.M. Puzikov, Chugai on effect of the bias electric field on the spectral distribution of the photo dielectric effect in the Schottky-barrier structures based on the Cadmium-zinc telluride crystals. *Semiconductors*, 41 (2007) 689-695.

[20] S. Barman, N.V. Venkataraman, S. Vasudevan, et al. Phase transitions in the anchored organic bilayers of long-chain alkylammonium lead iodides $(C_nH_{2n+1}NH_3)_2PbI_4$; $n=12, 16, 18$ [J]. *J.Phys. Chem. B* 107 (2003) 1875 - 1883.

[21] N. Kitazawa, Y. Watanabe, Nakamura Optical properties of $CH_3NH_3PbX_3$ (X= halogen) And their mixed-halide crystals [J]. *J. Mater. Sci.*, 37 (2002) 3585-3587.

[22] N. Mercier, S. Poiroux, A. Riou, et al. Unique hydrogen bonding correlating with a reduced band gap and phase transition in the hybrid perovskites $(HO(CH_2)_2NH_3)_2PbX_4$ (X = I, Br), [J].*Inorg. Chem.*, 43 (2004) 8361-8366

[23] D.B. Mitzi, Synthesis, Crystal structure, and optical and thermal properties of $(C_4H_9NH_3)_2ML_4$ (M= Ge, Sn, Pb), [J]. *Chem. Mater.*, 8 (1996) 791-800.

[24] T. Dammak, M, Koubaa, K. Boukheddaden, et al. Two-dimensional excitons and photoluminescence properties of the organic/inorganic $(4-FC_6H_4C_2H_4NH_3)_2[PbI_4]$. *Nanomaterial* [J]. *J. Phys. Chem. C*, 113 (2009)

19305-19309.

[25] R. Zheng, G. Wu, M. Deng, et al. Preparation and characterization of a layered perovskite-type organic-inorganic hybrid compound $(\text{C}_6\text{NH}_6\text{-CH}_2\text{CH}_2\text{NH}_3)_2\text{CuC}_{14}$ [J]. *Thin Solid Films*, 514 (2006) 127-131.

[26] S. Barman, S. Vasudevan, Melting of an anchored bilayer: phase transitions in the organic-inorganic hybrid perovskite $(\text{CH}_3\text{NH}_3)(\text{CH}_3(\text{CH}_2)_n\text{NH}_3)_2\text{Pb}_2\text{I}_7$ ($n = 11, 13, 15, 17$) [J]. *J. Phys. Chem. C*, 113 (2009) 15698-15706.

[27] D.B. Mitzi, K. Liang, Preparation and properties of $(\text{C}_4\text{H}_9\text{NH}_3)_2\text{EuI}_4$: A luminescent Organic-inorganic perovskite with a divalent rare-earth metal halide framework [J]. *Chem. Mater.*, 9 (1997) 2990-2995.

[28] Z. Xiao, Preparation and Properties of Ordered Materials Based on Linear Alkylamine Hybrid Calcium Structures [D]. Zhejiang University Learning, 2005.

[29] T. Hattori, T. Taira, M. Era, et al. Highly efficient electroluminescence from a heterostructure Device combined with emissive layered-perovskite and an electron-transporting organic Compound [J]. *Chem. Phys. Lett.*, 254 (1996) 103-108.

[30] J. Guan, Syntheses, characterization, properties of organic-inorganic perovskite compound. Ph D, thesis, University of Houston, USA, 2001.

[31] S.L Suib, P.F Weller, Gel growth of single crystals of some rubidium and cesium tin halides [J]. *Cryst. Growth*. 48 (1980) 51-56.

[32] D.B. Mitzi, A layered solution crystal growth technique and the crystal structure of $(\text{C}_6\text{HSC}_2\text{H}_4\text{NH}_3)_2\text{PbC}_{14}$ [J]. *J. Solid State Chem.*, 145 (1999) 694-704.

- [33] M. Era, T. Hattori, T. Taira, et al. Self-organized growth of PbI-based layered perovskite quantum well by dual-source vapor deposition [J]. Chem. Mater., 9 (1997) 10.
- [34] D.B. Mitzi, Templating and structural engineering in organic-inorganic perovskites. 1 (2001), 12.
- [35] K. Liang, D.B. Mitzi, M.T. Prikas, Synthesis and characterization of organic-inorganic Perovskite thin films prepared using a versatile two-step dipping technique [J]. Chem. Mater., 10 (1998) 403-411.
- [36] Y. Takeoka, M. Fukasawa, T. Matsui, et al. Intercalated formation of two-dimensional and multi-layered perovskites in organic thin films [J]. Chem. Commun., (2005) 378-380.
- [37] Y. Xia, White sides GM. Soft lithography. annul. Rev. Mater. Sci., 28 (1998) 153-84.
- [38] Z. Cheng, Z. Wang, R. Xing, et al. Patterning and photoluminescent properties of perovskite-type organic/inorganic hybrid luminescent films by soft lithography [J]. Chem., Phys. Lett., 376 (2003) 481-486.
- [39] S. Luan, Z. Cheng, X. Xing, et al. Patterning organic luminescent materials by solvent-assisted dewetting and polymer-bonding lithography. J. Appl. Phys., 97 (2005) 086102-3.
- [40] Y. Takeoka, K. Asai, M. Rikukawa, et al. Incorporation of conjugated polydiacetylene systems into organic-inorganic quantum-well structures [J]. Chem. Commun., 24 (2001) 592-2-593.
- [41] M. Morita, M. Kameyama, Exchange effects on the luminescence of

the quasi two dimensional anti ferro magnet $(\text{C-H}_2\text{-+1NH}_3)\text{ZMnCl}_4$ ($n=1, 2, 3$) [J]. J. Lumin., 24 (1981) 79-82.

[42] M. Era, S. Morimoto, T. Tsutsui, et al. Organic-inorganic heterostructure electro luminescent device using a layered perovskite semiconductor $(\text{C}_6\text{H}_5\text{C}_2\text{H}_4\text{NH}_3)_2\text{PbI}_4$ [J]. Appl. Phys. Lett., 65 (1994) 576-578.

[43] K. Chondroudis, D.B. Mitzi Electroluminescence from an organic-inorganic perovskite incorporating a quarter thiophene dye within lead halide perovskite layers [J]. Chem. Mater. 11 (1999) 3028-3030.

[44] C.R. Kagan, D.B. Mitzi, C.D. Dimitrakopoulos, Organic-inorganic hybrid materials as semiconducting channels in thin-film field-effect transistors [J]. Science, 28694 (1999) 947.

[45] D.B. Mitzi, C.D. Dimitrakopoulos, J. Rosner, et al. Hybrid field-effect transistor based on a low-temperature melt-processed channel layer [J]. Adv. Mater., 14 (2002) 1772-1776.

[46] K. Ema, M. Inomata, Y. Kato, et al. Nearly perfect triplet-triplet energy transfer from Wannier excitons to naphthalene in organic-inorganic hybrid quantum-well materials [J]. Phys. Rev. Lett., 100 (2008) 257401.

[47] K. Shibuya, M. Koshimizu, Y. Takeoka, et al. Scintillation properties of $(\text{C}_6\text{H}_{13}\text{NH}_3)_2\text{PbI}_4$: Exciton luminescence of an organic/inorganic multiple quantum well structure compound induced by 2.0 meV protons [J]. Phys. Res. B, 194 (2002) 207-212.

[48] V.G. Mayorov, A.I. Nikolaev, L.A. Safonova, Investigation of conditions for extraction separation of thorium from calcium and

lanthanum. Theoretical Foundations of Chemical Engineering, 43(2009) 831-833.

[49] R.D Mills, J.J Ratner, A.F Glazner, Experimental evidence for crystal coarsening and fabric development during temperature cycling. Geology 39 (2011) 1139-1142.

[50] N. Mercier, S. Poiroux, A. Riou, et al. Unique hydrogen bonding correlating with a reduced band gap and phase transition in the hybrid perovskites $(\text{HO}(\text{CH}_2)_2\text{NH}_3)_2\text{PbX}_4$ ($\text{X} = \text{I}, \text{Br}$) Inorg. Chem., 43 (2004) 8361-8366.

[51] Z. Cheng, J.L. Lin organic-inorganic hybrid perovskites: structure, optical properties, film preparation, patterning and templating engineering [J]. Cryst. Eng. Comm., 12 (2010) 2646-2662

[52] K. Pradeesh, J.J Baumberg, G.V. Prakash. In situ intercalation strategies for device-quality hybrid inorganic-organic self-assembled quantum wells [J]. Appl. Phys. Lett., 95 (2009) 033309

[53] T. Liu, G. Yang, W. Chun. Side chain and solvation effects on the photophysical properties of fluorene-alt-benzene based conjugated block copolymers. Acta Chimica Sinica 69 (2011) 1424.

[54] L. Rocchigiani, G. Bellachioma, C. Gianluca, et al. Synthesis, characterization, interionic structure, and self-aggregation tendency of zircon aziridinium salts bearing long alkyl chains. Organometallics 30 (2011) 100-114.

[55] C. Li, H. Deng, J. Wan, et al. Photoconductive properties of organic-inorganic hybrid perovskite $(\text{C}_6\text{H}_{13}\text{NH}_3)_2(\text{CH}_3\text{NH}_3)_{m-1}\text{Pb}_m\text{I}_{3m+1}:\text{TiO}_2$ nanocomposites device structure 64 (2010) 2735-2737.

[56] L. Zhou, F. Zhang, Thermo-sensitive and photoluminescent hydrogels: synthesis, characterization, and their drug-release property. *Materials Science & Engineering C*, 31 (2011) 1429-1435.

